非線形構造形成

解析的アプローチ

Contents

- 球対称コラプスモデル
- ゼルドビッチ近似と高次摂動
- オイラー的摂動論

球対称コラプスモデル

(Spherical collapse model, SCM)

Halo formation

Halo 1 (M~10^15 M_sun/h) Suto, Kitayama, Osato, Sasaki & Suto (16)

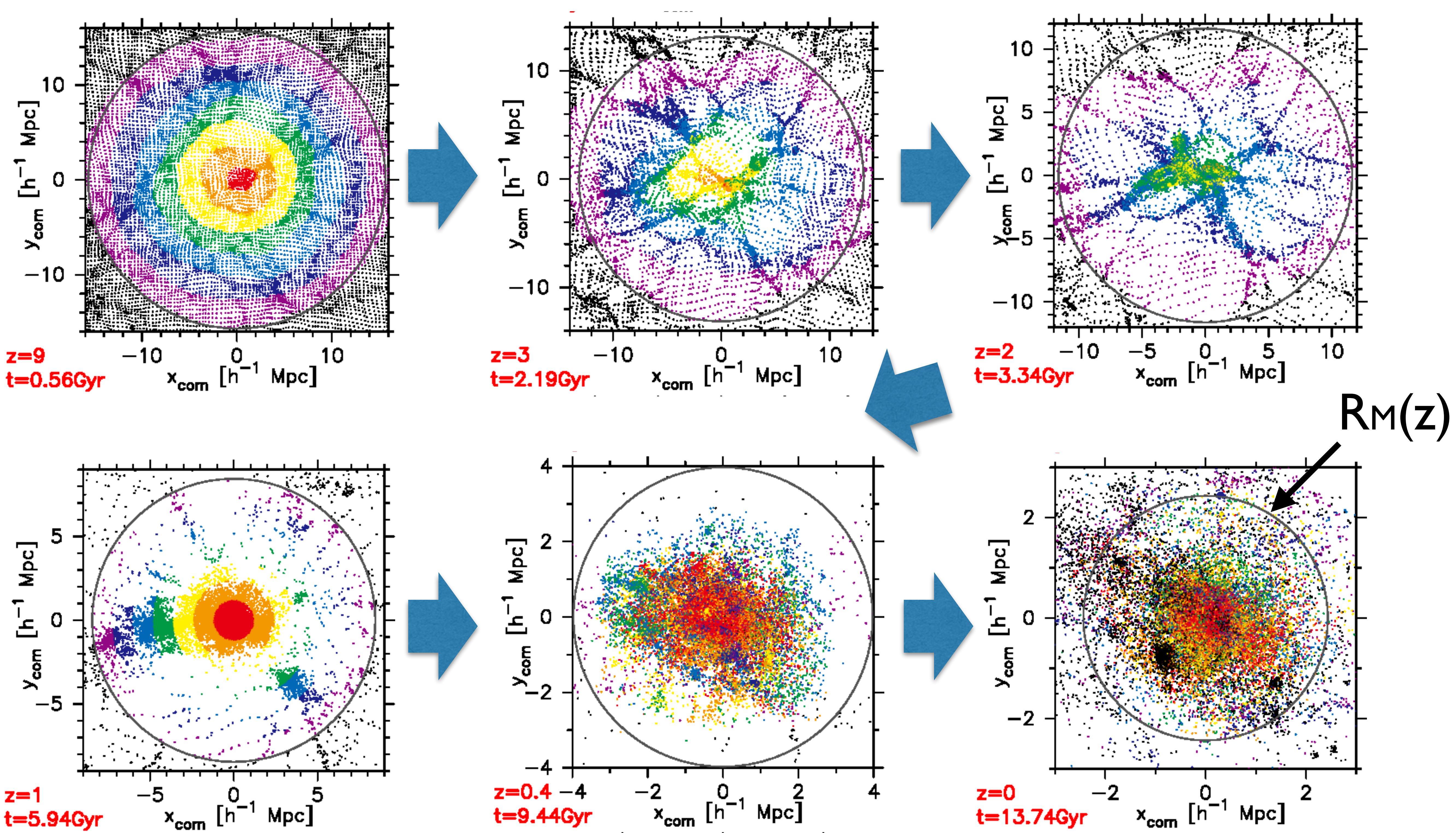

Comparison with SCM

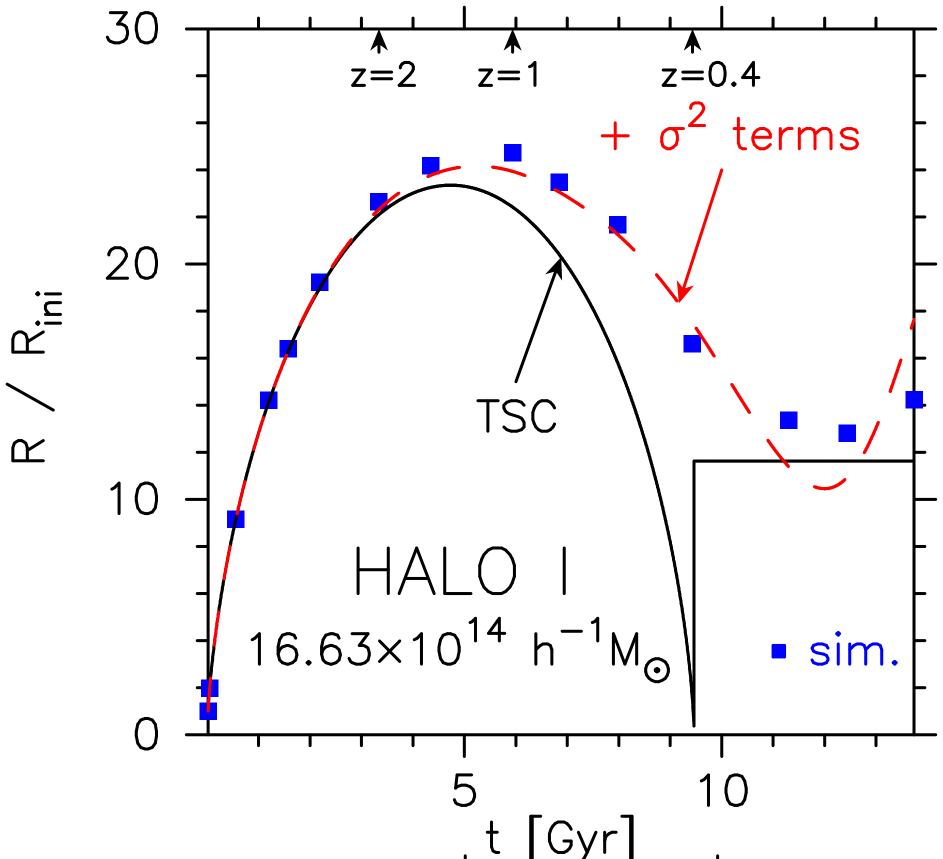

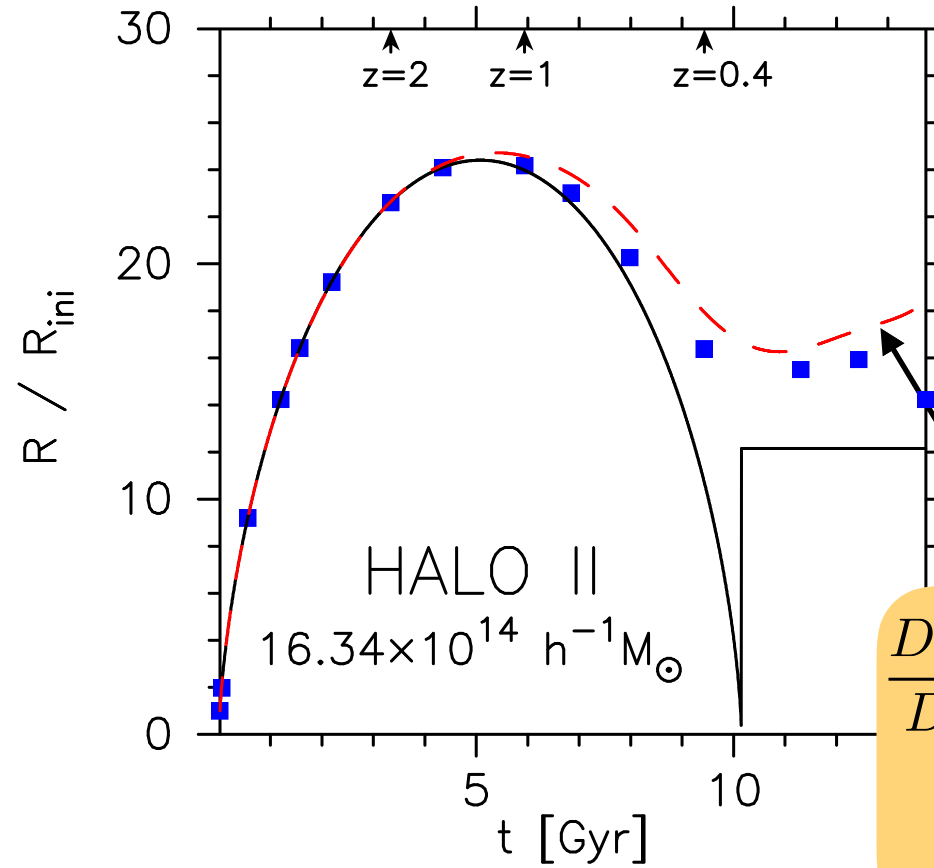

Evolution of

$R_M(z)$

$$\frac{Dv_r}{Dt} = -\frac{1}{\rho}\frac{\partial(\rho\sigma_r^2)}{\partial r} - \frac{2\sigma_r^2 - \sigma_{\rm tan}^2}{r} - \frac{GM}{r^2}$$

(Jeans eq.)

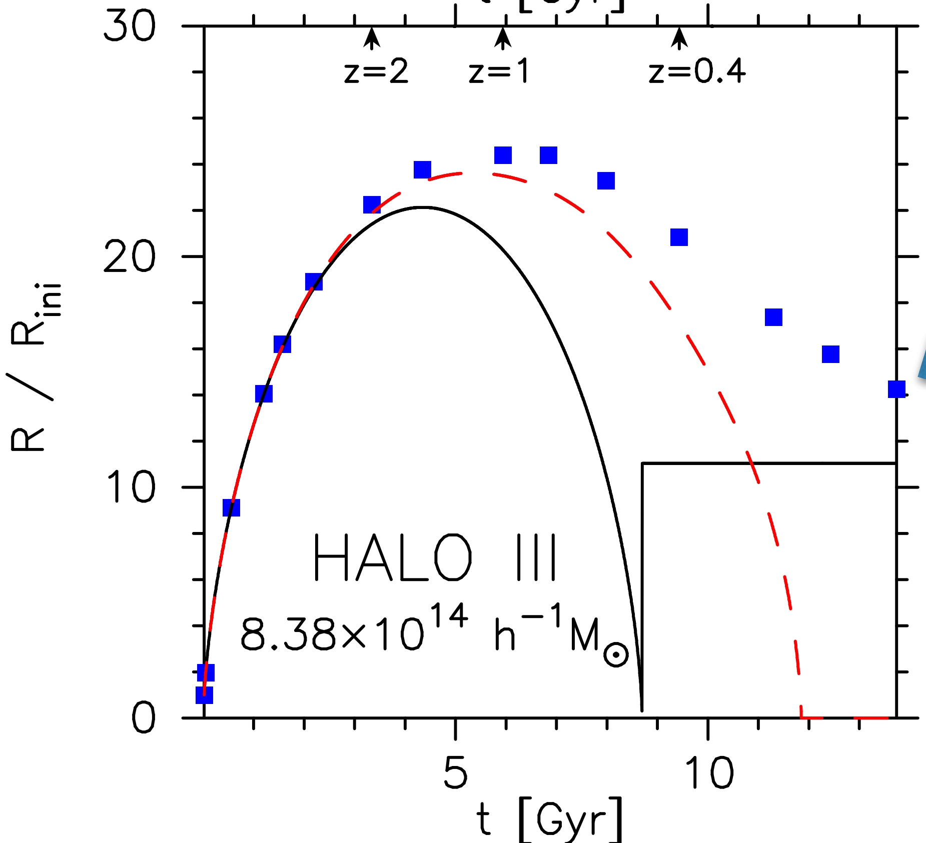

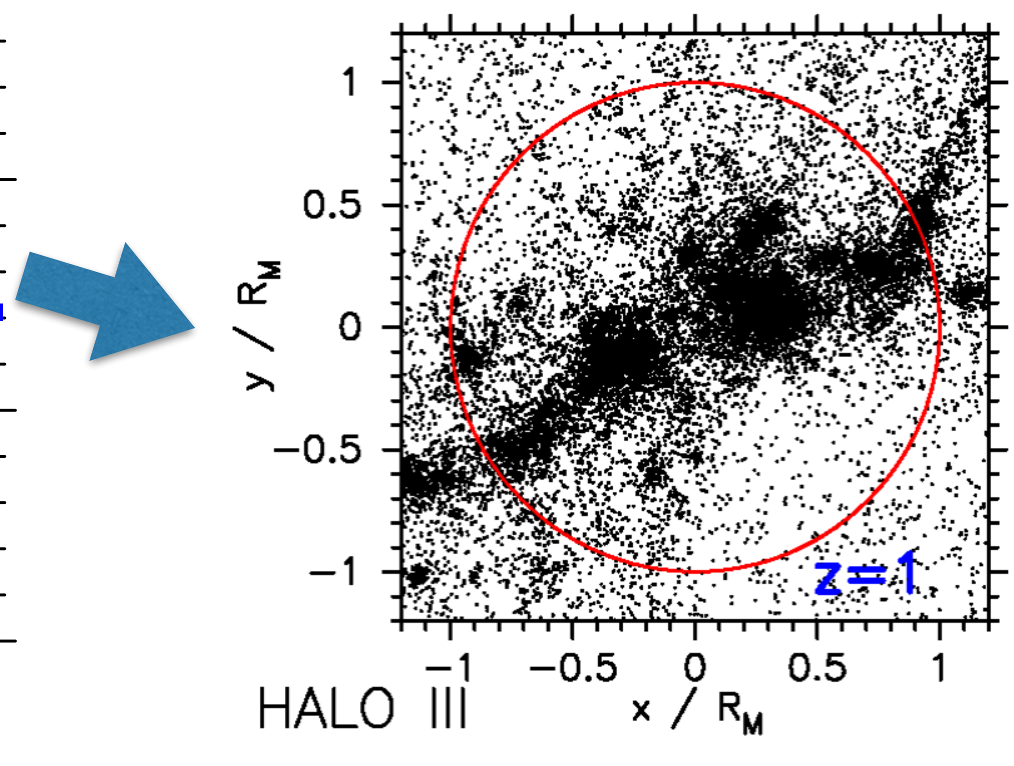

Suto, Kitayama, Osato, Sasaki & Suto (16)

Beyond spherical collapse model (SCM)

SCM only describes the onset of halo formation

In particular, SCM fails to describe phase-space structure of halo (continuous matter accretion)

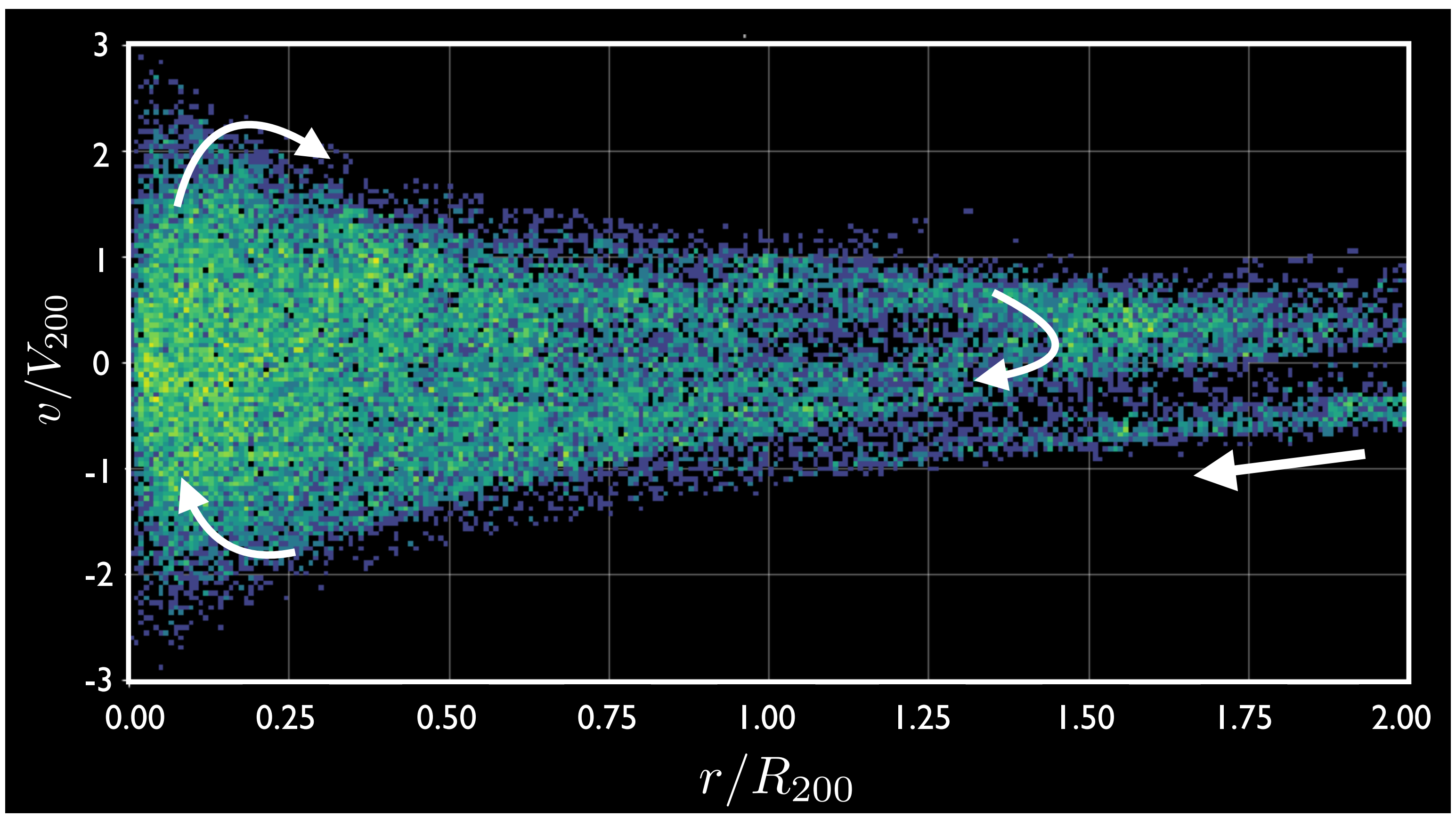

Tractable analytic treatment

Self-Similar collapse

e.g., Fillmore & Goldreich ('84)
Bertschinger ('85)

Self-similar collapse

Fillmore & Goldreich ('84)

- Einstein-de Sitter background, $a(t) \propto t^{2/3}$
- Scale-free initial density perturbation, $\delta_{\rm i} \propto M_{\rm i}^{-\epsilon}$
- Motion of continuously infall shells at $r < r_*$

turn-around radius

Self-similar ansatz

$$r(t, t_*) = r_*(t_*)\lambda(t/t_*)$$

$$\Lambda(\tau) = \tau^{2/3+2/9\varepsilon}$$

EoM

$$\frac{d^2\lambda}{d\tau^2} = -\frac{\pi^2}{8}\frac{\tau^{2/3\varepsilon}}{\lambda^2}\mathscr{M}\left[\frac{\lambda}{\Lambda(\tau)}\right] \ ; \ \mathscr{M}(x) = \frac{2}{3\varepsilon}\int_1^\infty \frac{dy}{y^{1+2/3\varepsilon}} \underline{\mathscr{H}\left[x - \frac{\lambda(y)}{\Lambda(y)}\right]}$$

$\tau \equiv t/t_*$: time normalized by turn-around time

Heaviside step func.

Mass: $M(r,t) = M_t\, \mathcal{M}\left(\dfrac{\lambda}{\Lambda(t)}\right)$; $M_t \propto a(t)^{1/\epsilon}$

Solutions

修論 by 杉浦宏夢

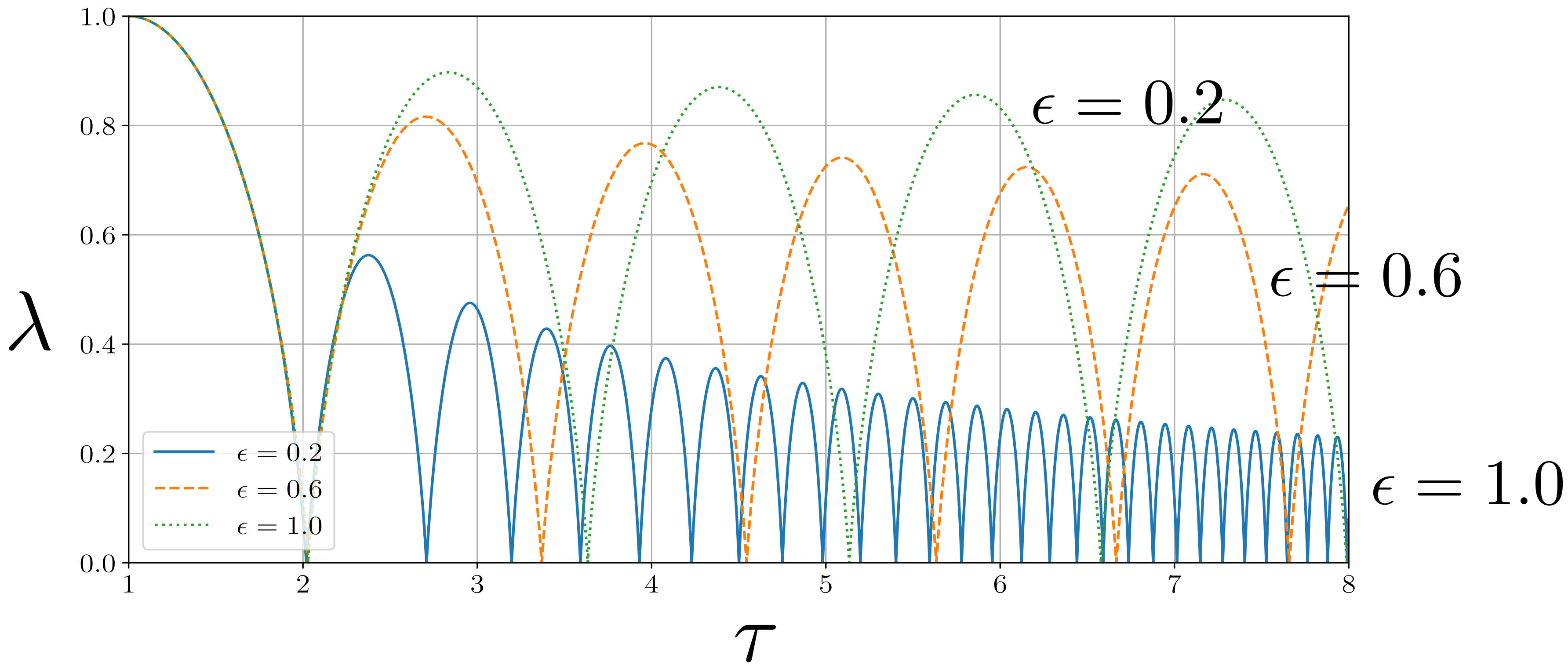

trajectory of mass shell

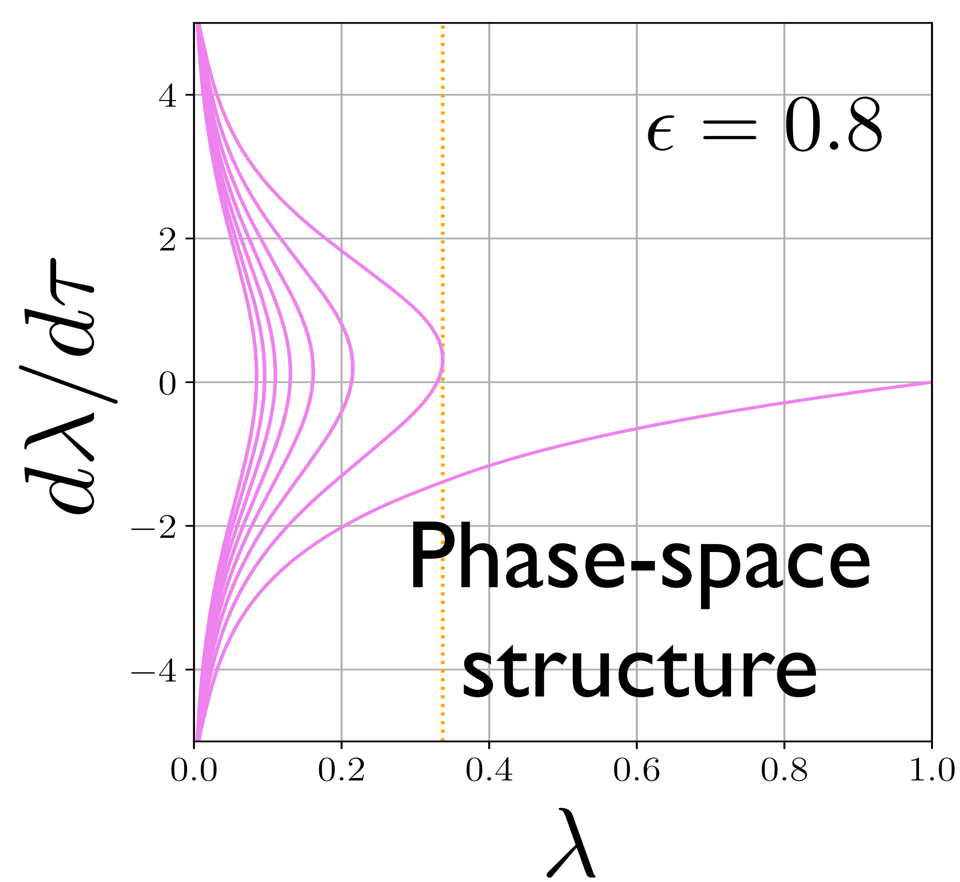

Phase-space structure

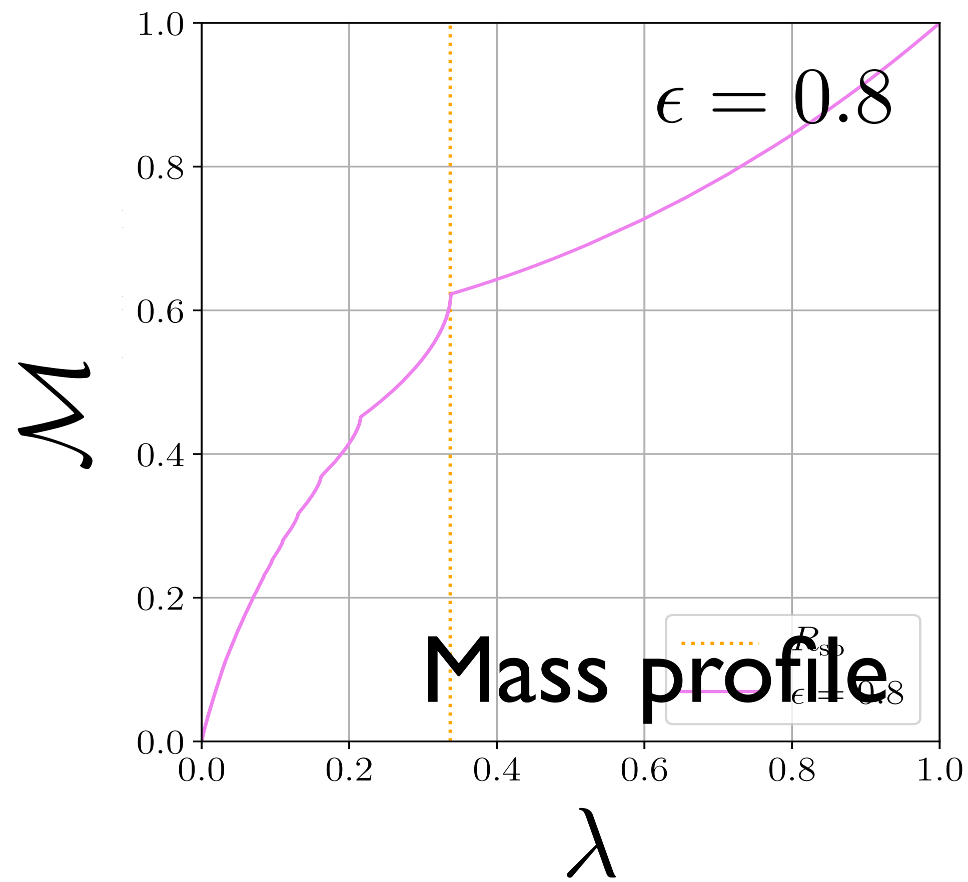

Mass profile

Tracing multi-stream flow with particle trajectories in *N*-body simulation

修論 by 杉浦宏夢

Keeping track of apocenter passage(s) for particle trajectories,

number of apocenter passages, p, is stored for each particle

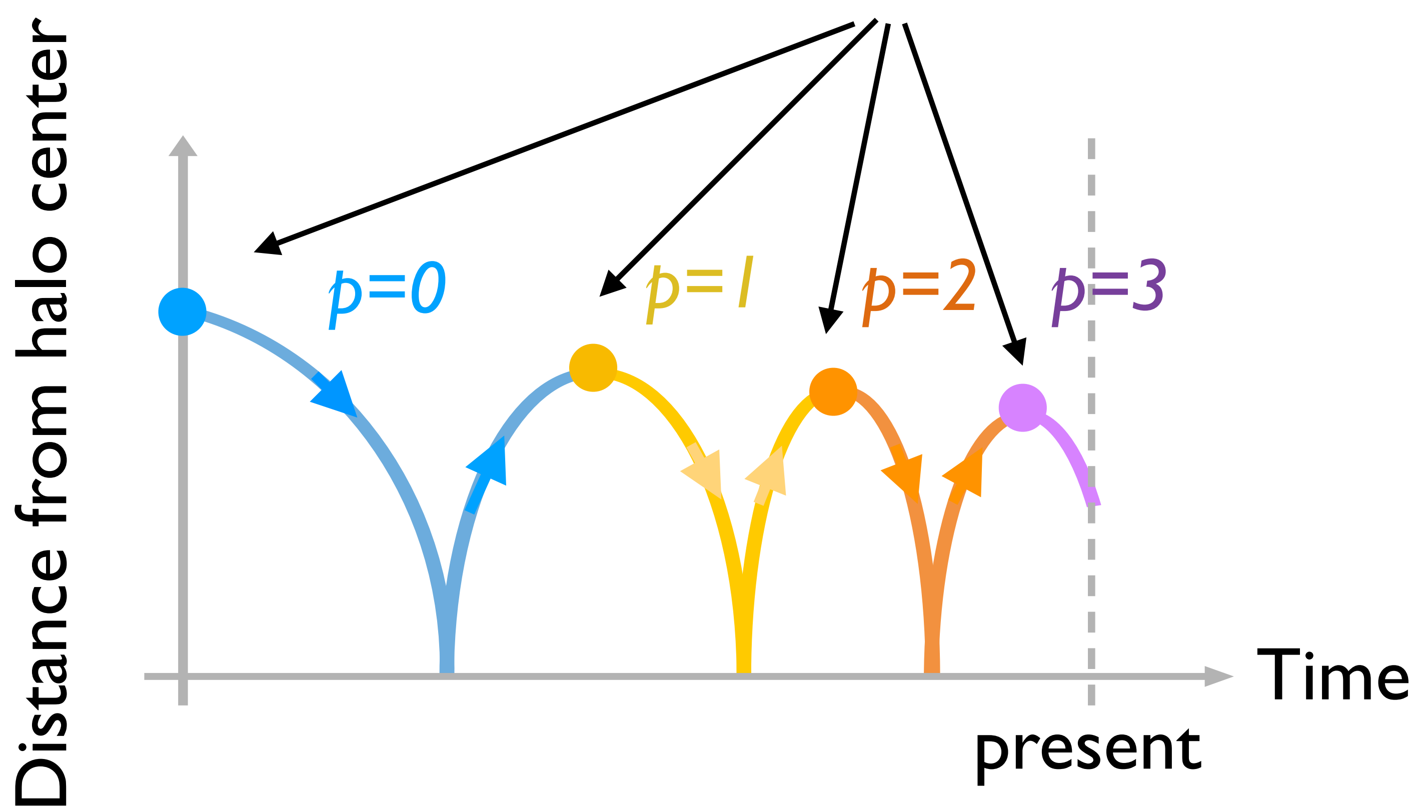

= SPARTA algorithm + α

(Diemer'17; Diemer et al.'17)

Tiling phase-space streams with p

N-body simulation

Y. Rasera@

(Observatoire de Paris)

- L=316Mpc/h, N=512^3
- 60 snapshots at 0<z<1.43
- Einstein-de Sitter universe

11,000 halos

$(M_{200} \geq 10^{13} M_\odot)$

Comparison with self-similar solution

Use apocenter-passage positions
p=1~5 to fit to self-similar solution
by Fillmore & Goldreich ('84)

Fitting parameters:

$$s = (1/\epsilon), \quad r_{\mathrm{ta}}(t_{\mathrm{ta}})$$

accretion rate $(M \propto a^s)$ scale radius

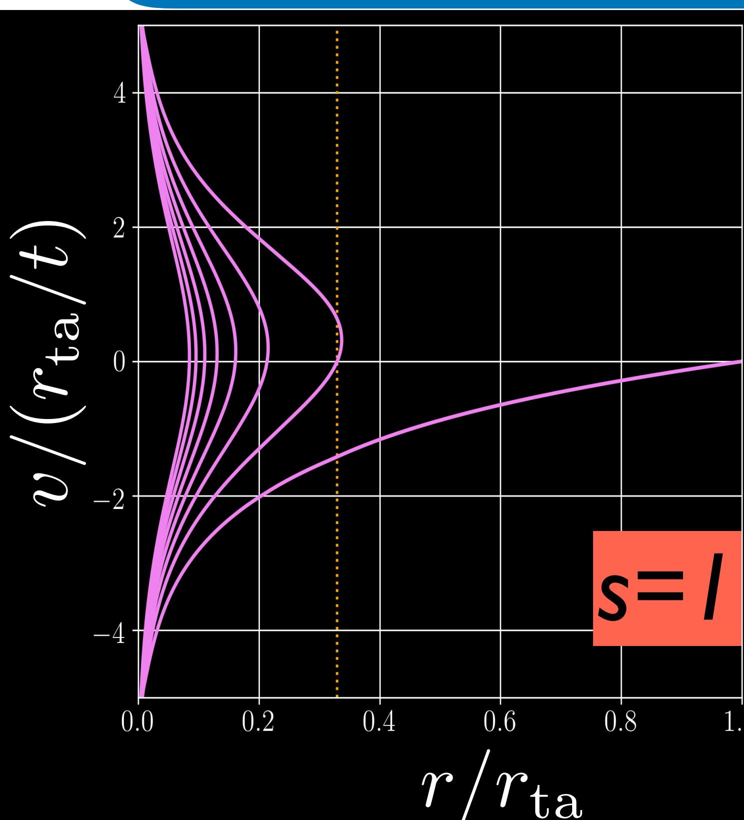

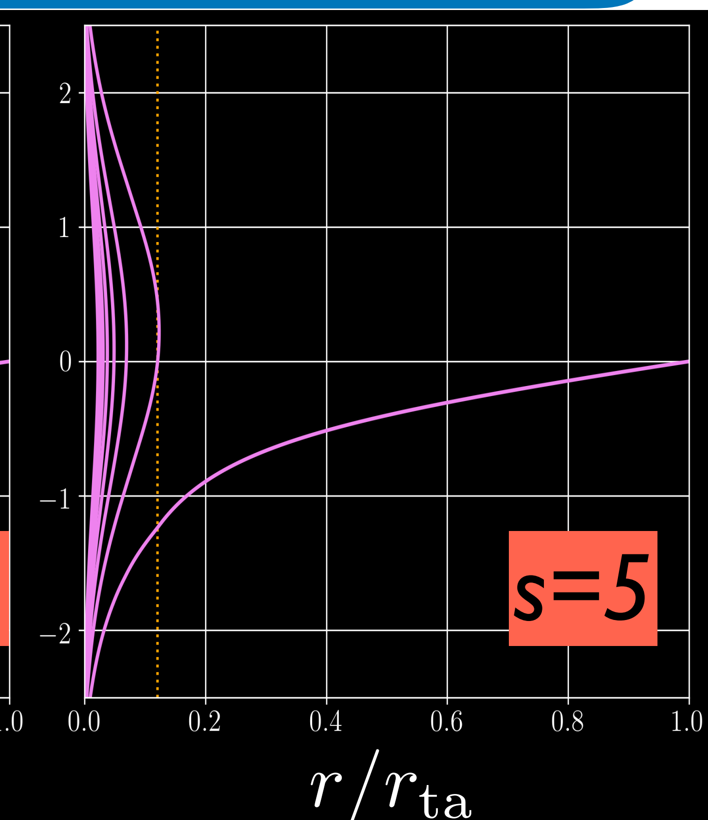

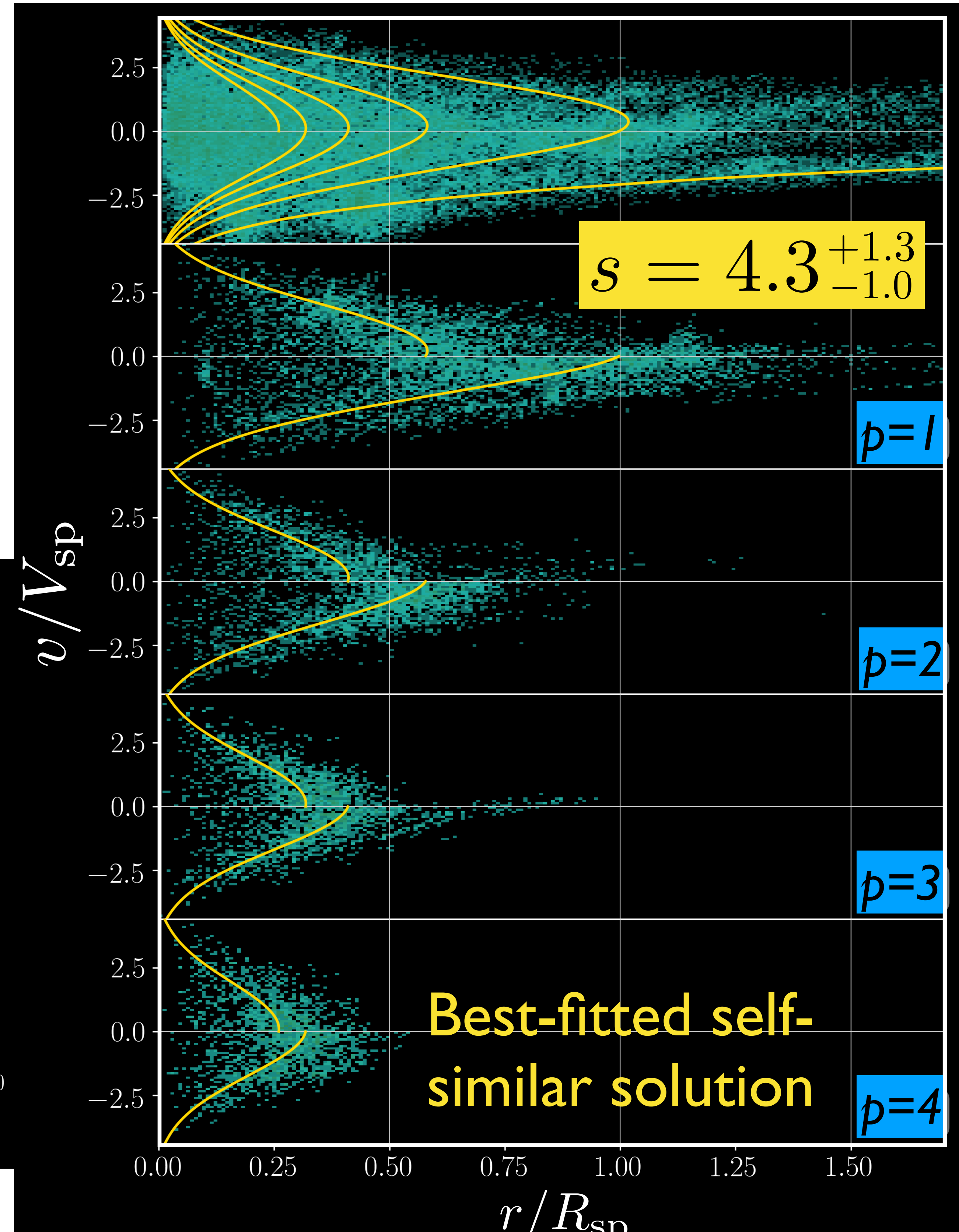

(Master thesis by H. Sugiura)

Zel’dovich近似と高次摂動
（ラグランジェ摂動論）

Lagrangian PT

Basic equations

$$L = \frac{1}{2}\, m\, a^2 \dot{\boldsymbol{x}}^2 - m\, \phi(\boldsymbol{x})$$

$$\ddot{\boldsymbol{x}} + 2H\dot{x} = -\frac{1}{a^2}\, \nabla_x\, \phi(\boldsymbol{x}),$$

$$\nabla_x^2\, \phi(\boldsymbol{x}) = 4\pi\, G a^2 \overline{\rho}_{\mathrm{m}}\, \delta(\boldsymbol{x}).$$

Lagrangian coordinate (***q***): $\boldsymbol{x}(\boldsymbol{q},t) = \boldsymbol{q} + \boldsymbol{\Psi}(\boldsymbol{q},t)$

In Lagrangian coordinate, mass density is assumed to be uniform:

$$\overline{\rho}_{\mathrm{m}}\, d^n\boldsymbol{q} = \rho_{\mathrm{m}}(\boldsymbol{x})\, d^n\boldsymbol{x} \longrightarrow \delta(\boldsymbol{x}) = \frac{\rho_{\mathrm{m}}(\boldsymbol{x})}{\overline{\rho}_{\mathrm{m}}} - 1 = \left|\frac{\partial \boldsymbol{x}}{\partial \boldsymbol{q}}\right|^{-1} - 1$$

Rewriting quantities in Eulerian space with those in Lagrangian quantities

Lagrangian PT

Matsubara ('15)

$$\nabla_x \cdot \left[\ddot{\boldsymbol{x}} + 2H\dot{\boldsymbol{x}}\right] = -4\pi\,G\,\overline{\rho}_{\rm m}\,\delta,$$

$$\nabla_x \times \left[\ddot{\boldsymbol{x}} + 2H\dot{\boldsymbol{x}}\right] = \boldsymbol{0}.$$

$$\hat{\mathcal{T}} f(t) \equiv \ddot{f}(t) + 2H\dot{f}(t)$$

Longitudinal: $\left(\hat{\mathcal{T}} - 4\pi\,G\,\overline{\rho}_{\rm m}\right)\Psi_{k,k}$

$$= -\epsilon_{ijk}\epsilon_{ipq}\,\Psi_{j,p}\left(\hat{\mathcal{T}} - 2\pi\,G\,\overline{\rho}_{\rm m}\right)\psi_{k,q}$$

$$- \frac{1}{2}\epsilon_{ijk}\epsilon_{pqr}\,\Psi_{i,p}\Psi_{j,q}\left(\hat{\mathcal{T}} - \frac{4\pi\,G}{3}\,\overline{\rho}_{\rm m}\right)\Psi_{k,r},$$

Transverse: $\epsilon_{ijk}\,\hat{\mathcal{T}}\,\Psi_{j,k} = -\epsilon_{ijk}\,\Psi_{p,j}\hat{\mathcal{T}}\Psi_{p,k}.$

Levi-Civita symbol

PT expansion: $\boldsymbol{\Psi}(\boldsymbol{q},\,t) = \boldsymbol{\Psi}^{(1)}(\boldsymbol{q},\,t) + \boldsymbol{\Psi}^{(2)}(\boldsymbol{q},\,t) + \boldsymbol{\Psi}^{(3)}(\boldsymbol{q},\,t) + \cdots$

Zel'dovich solution: 1st-order LPT

$$\boldsymbol{\Psi}^{(1)} = \boldsymbol{\Psi}^{(1L)} + \boldsymbol{\Psi}^{(1T)} \ \ ;$$

$\eta \equiv \ln D_1(t)$

$$\left(\frac{\partial^2}{\partial\eta^2} + \frac{1}{2}\frac{\partial}{\partial\eta} - \frac{3}{2}\right)\Psi^{(1L)}_{k,k} = 0$$

$$\left(\frac{\partial^2}{\partial\eta^2} + \frac{1}{2}\frac{\partial}{\partial\eta}\right)\epsilon_{ijk}\Psi^{(1T)}_{j,k} = 0$$

Zel'dovich approximation : $\boldsymbol{\Psi}^{(1T)} = 0$ and take growing-mode only

$$\boldsymbol{\Psi}^{(1)} = \boldsymbol{\Psi}^{(1L)} = -\,D_1(a)\,\nabla_q\varphi(\boldsymbol{q}), \qquad \nabla_q^2\varphi(\boldsymbol{q}) = \delta_0(\boldsymbol{q})$$

: initial density field

$$\because \quad 1+\delta_{\rm m}(\boldsymbol{x}) = \left|\frac{\partial\boldsymbol{x}}{\partial\boldsymbol{q}}\right|^{-1} \equiv \frac{1}{J} \simeq 1 - \nabla_q\cdot\boldsymbol{\psi}$$

Particle trajectories in ZA

ZA

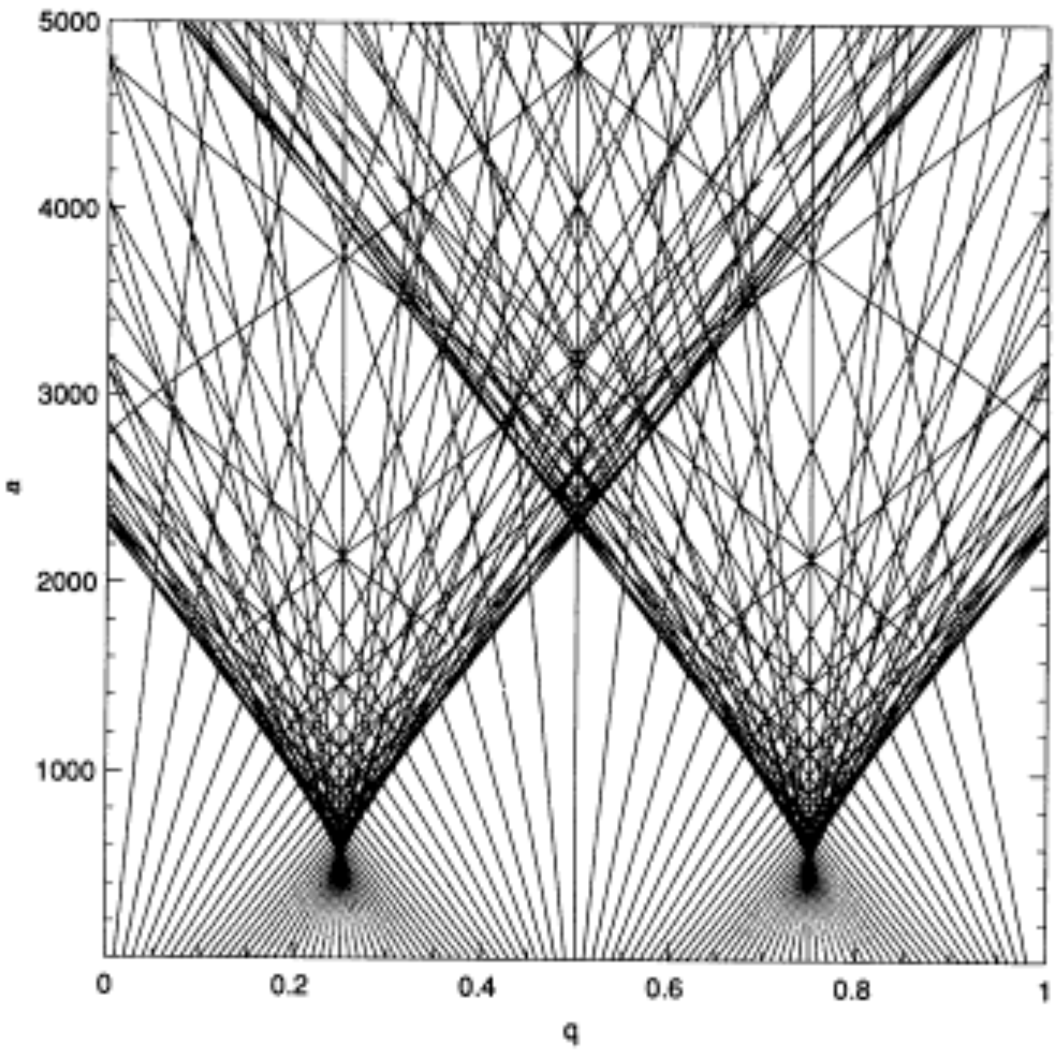

2LPT

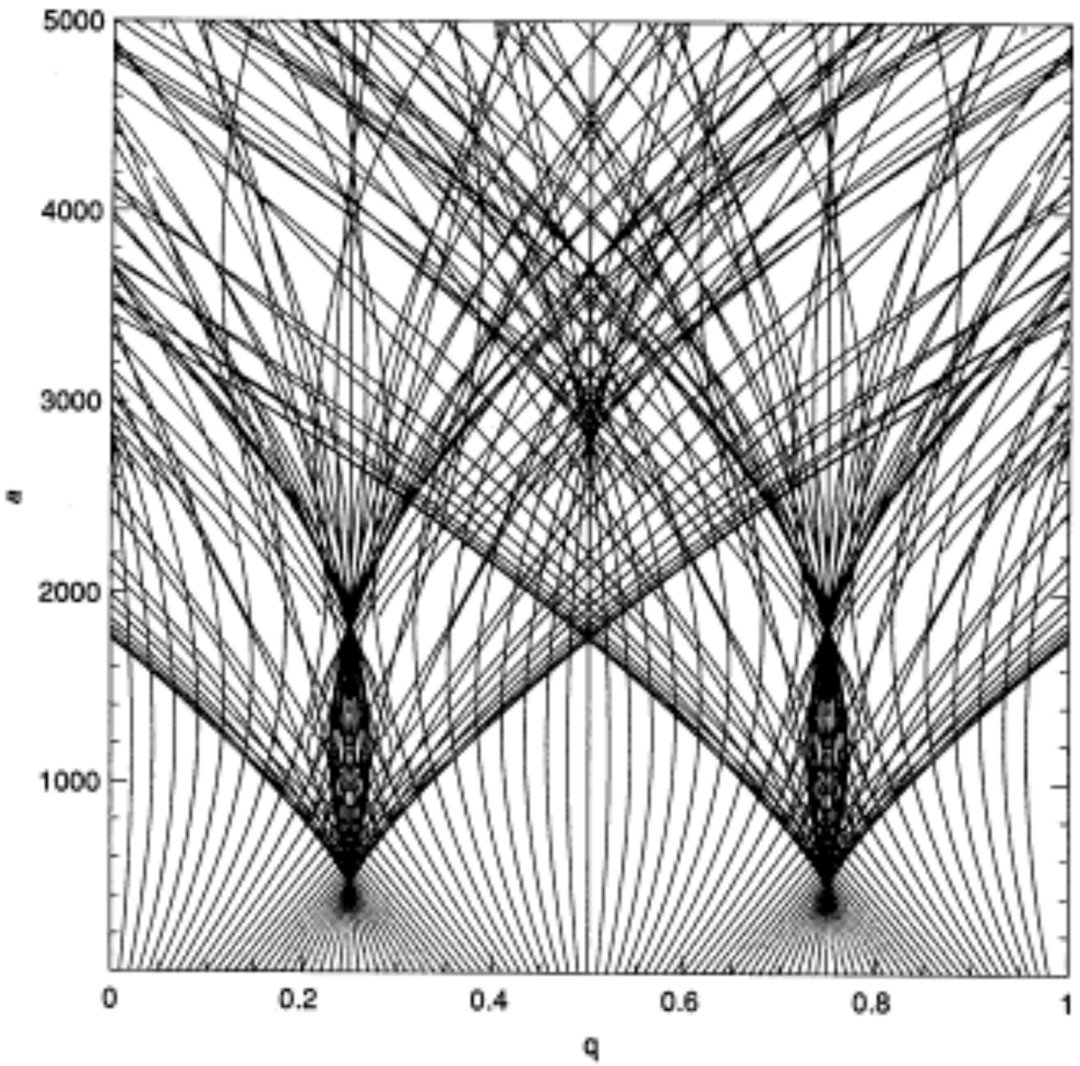

Figure 3. A family of trajectories corresponding to the model presented in Fig. 1 is shown for the first-order (upper panel) and second-order (lower panel) approximations. The trajectories end in the Eulerian space–time section ($y=0.5$, t) centred at a cluster. These plots illustrate that the three-stream system that develops after the first shell-crossing performs a self-oscillation due to the action of self-gravity.

Buchert & Ehlers ('93)

Full N-body | Zel'dovich | 2LPT

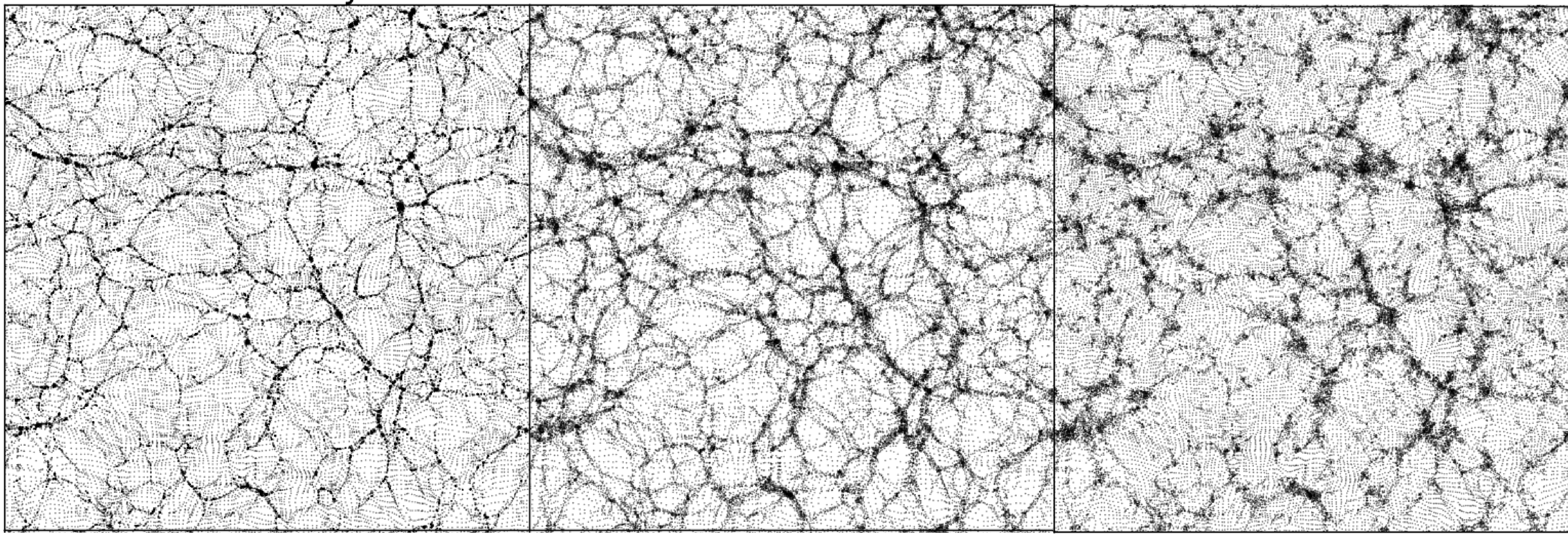

N_particle = 256^3

L=200Mpc/h

ΛCDM

Neyrink ('13)

power spectrum

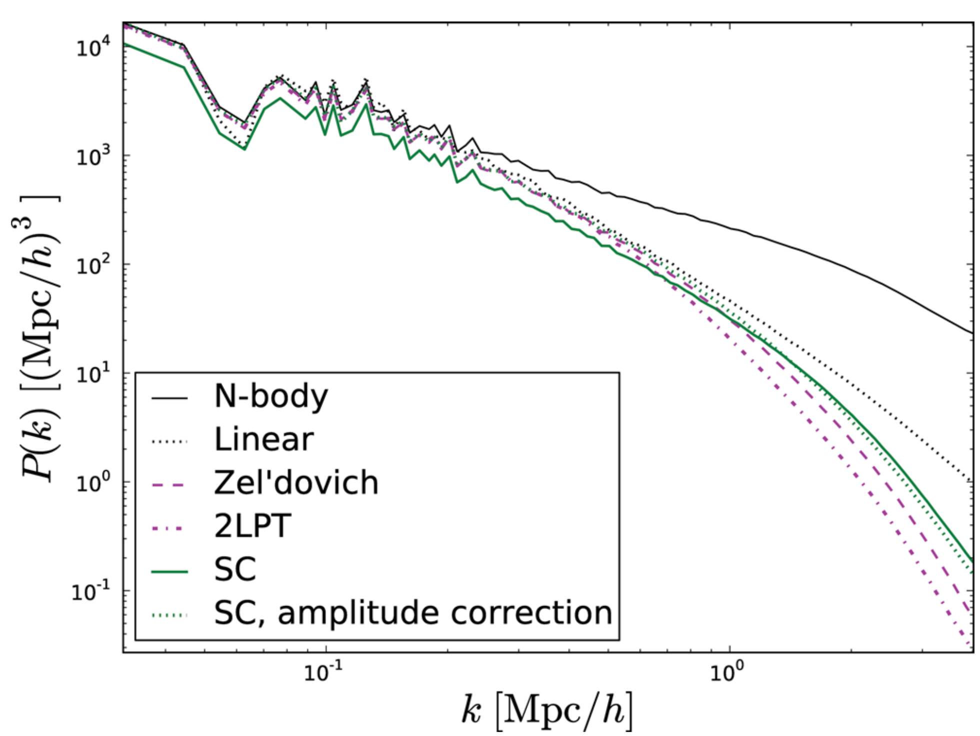

cross correlation coeff.

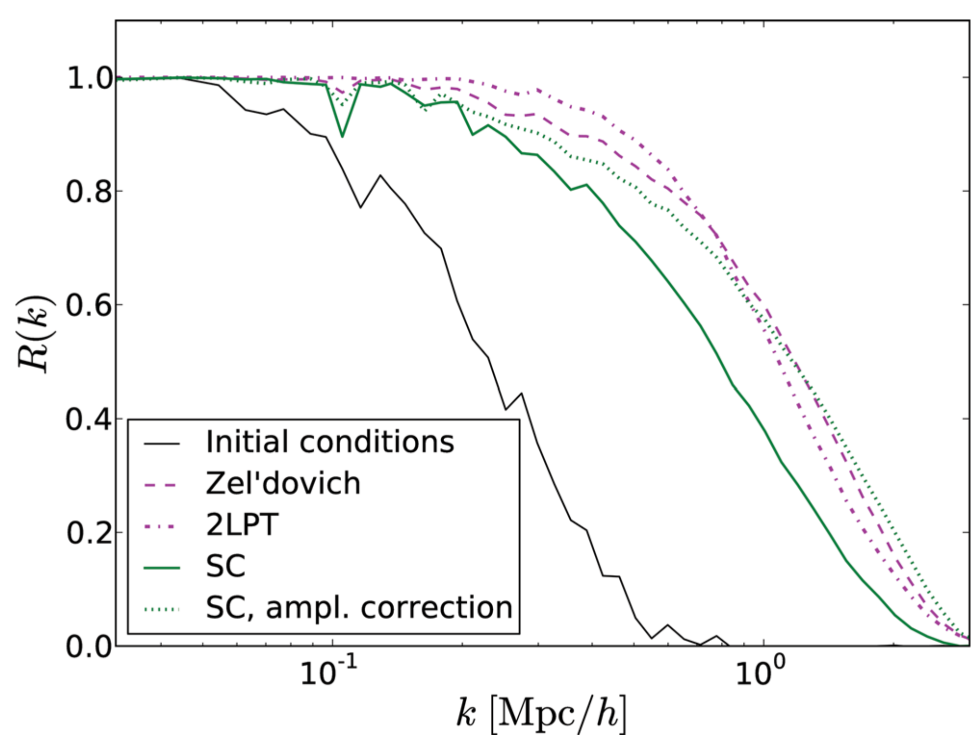

Zel'dovich近似の応用

N体シミュレーションの初期条件生成に有用

粒子を格子状に並べてZel'dovich近似でずらす：

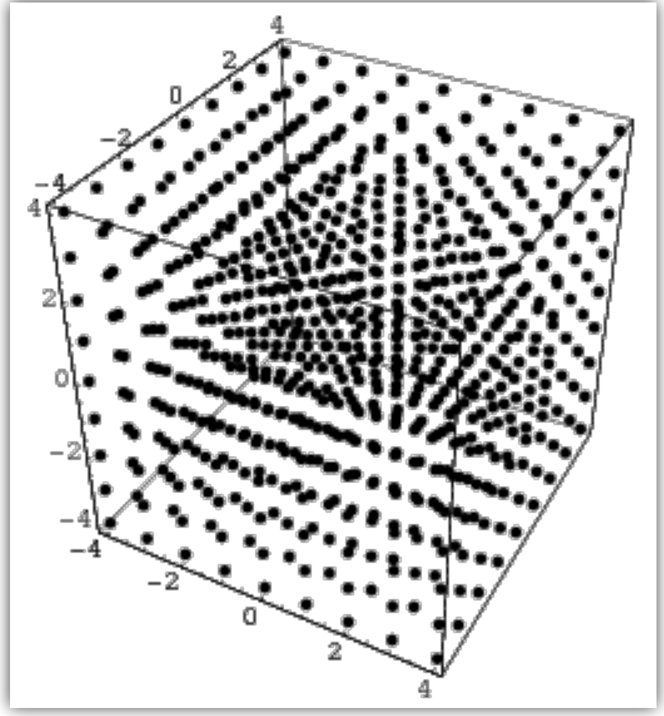

$$\boldsymbol{x} = \boldsymbol{q} + \boldsymbol{\Psi}(\boldsymbol{q}) \qquad \boldsymbol{v} = a\dot{\boldsymbol{x}} = a\dot{\boldsymbol{\Psi}}(\boldsymbol{q})$$

格子点の位置　変移場ベクトル

Zel'dovich近似：

$$\Psi(\boldsymbol{k}) \simeq \frac{i\,\boldsymbol{k}}{k^2} D_+(z)\,\delta_0(\boldsymbol{k})$$

初期密度ゆらぎ

計算の流れ

1. フーリエ空間上にランダムな初期密度場を生成 $\delta_0(\boldsymbol{k})$
2. 変移場ベクトルを計算： $\boldsymbol{\Psi}(\boldsymbol{k}) \xrightarrow{\text{FFT}} \boldsymbol{\Psi}(\boldsymbol{q})$
3. 変移場ベクトルを使って粒子を移動： $\boldsymbol{\Psi}(\boldsymbol{q}) \qquad \dot{\boldsymbol{\Psi}}(\boldsymbol{q}) = \frac{\dot{D}_+(z)}{D_+(z)}\boldsymbol{\Psi}(\boldsymbol{q})$

Higher-order Lagrangian PT

e.g,. Matsubara ('15)

PT expansion: $\boldsymbol{\Psi}(\boldsymbol{q},\,t)=\boldsymbol{\Psi}^{(1)}(\boldsymbol{q},\,t)+\boldsymbol{\Psi}^{(2)}(\boldsymbol{q},\,t)+\boldsymbol{\Psi}^{(3)}(\boldsymbol{q},\,t)+\cdots$

Under Einstein-de Sitter approximation: $\boldsymbol{\Psi}^{(n)}_{\text{EdS}}(\boldsymbol{q};\,a(t))\longrightarrow\boldsymbol{\Psi}^{(n)}(\boldsymbol{q};\,D_1(t))$

$\eta\equiv\ln D_1(t)$

Longitudinal:
$$\left(\frac{\partial^2}{\partial\eta^2}+\frac{1}{2}\frac{\partial}{\partial\eta}-\frac{3}{2}\right)\Psi^{(n)}_{k,k}$$
$$=-\sum_{m_1+m_2=n}\underline{\epsilon_{ijk}\epsilon_{ipq}\,\Psi^{(m_1)}_{j,p}\left(\frac{\partial^2}{\partial\eta^2}+\frac{1}{2}\frac{\partial}{\partial\eta}-\frac{3}{4}\right)\psi^{(m_2)}_{k,q}}$$

vanished in 1D

$$-\frac{1}{2}\sum_{m_1+m_2+m_3=n}\underline{\epsilon_{ijk}\epsilon_{pqr}\,\Psi^{(m_1)}_{i,p}\Psi^{(m_2)}_{j,q}\left(\frac{\partial^2}{\partial\eta^2}+\frac{1}{2}\frac{\partial}{\partial\eta}-\frac{1}{2}\right)\Psi^{(m_3)}_{k,r}},$$

vanished in 2D

Transverse:
$$\epsilon_{ijk}\left(\frac{\partial^2}{\partial\eta^2}+\frac{1}{2}\frac{\partial}{\partial\eta}\right)\Psi^{(n)}_{j,k}=-\sum_{m_1+m_2=n}\underline{\epsilon_{ijk}\,\Psi^{(m_1)}_{p,j}\left(\frac{\partial^2}{\partial\eta^2}+\frac{1}{2}\frac{\partial}{\partial\eta}\right)\Psi^{(m_2)}_{p,k}}.$$

vanished in 1D

Performance of Lagrangian PT

Saga, AT & Colombi, arXiv:1805.08787

初期条件
（Zel'dovich近似解）

$$\boldsymbol{\Psi}(\boldsymbol{q}) = a_{\rm init}\begin{pmatrix} \epsilon_{\rm x}\sin q_x \\ \epsilon_{\rm y}\sin q_y \\ \epsilon_{\rm z}\sin q_z \end{pmatrix}$$

10次まで計算

宇宙論的ヴラソフシミュレーションと比較

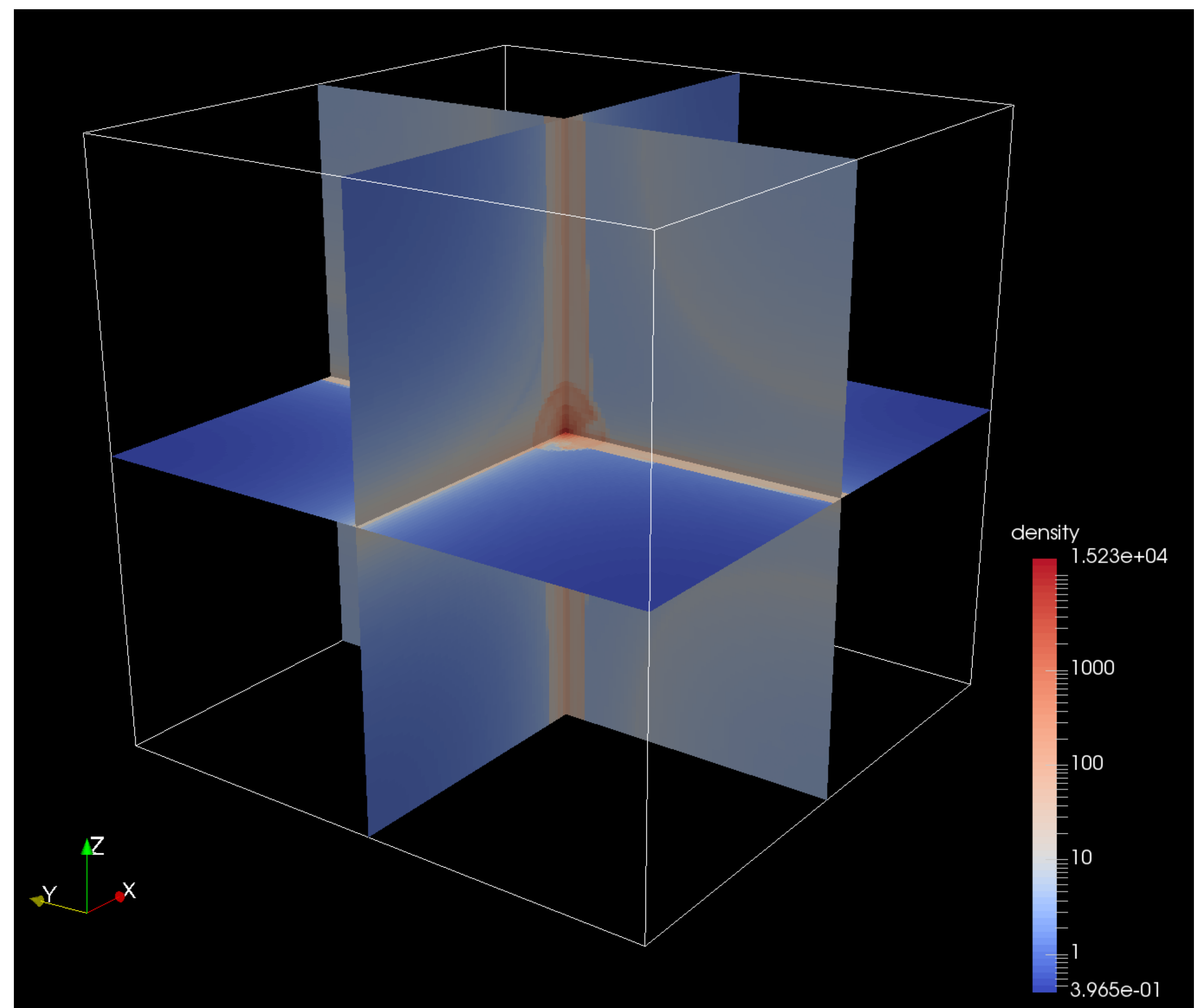

Results

Saga, AT & Colombi, arXiv:1805.08787

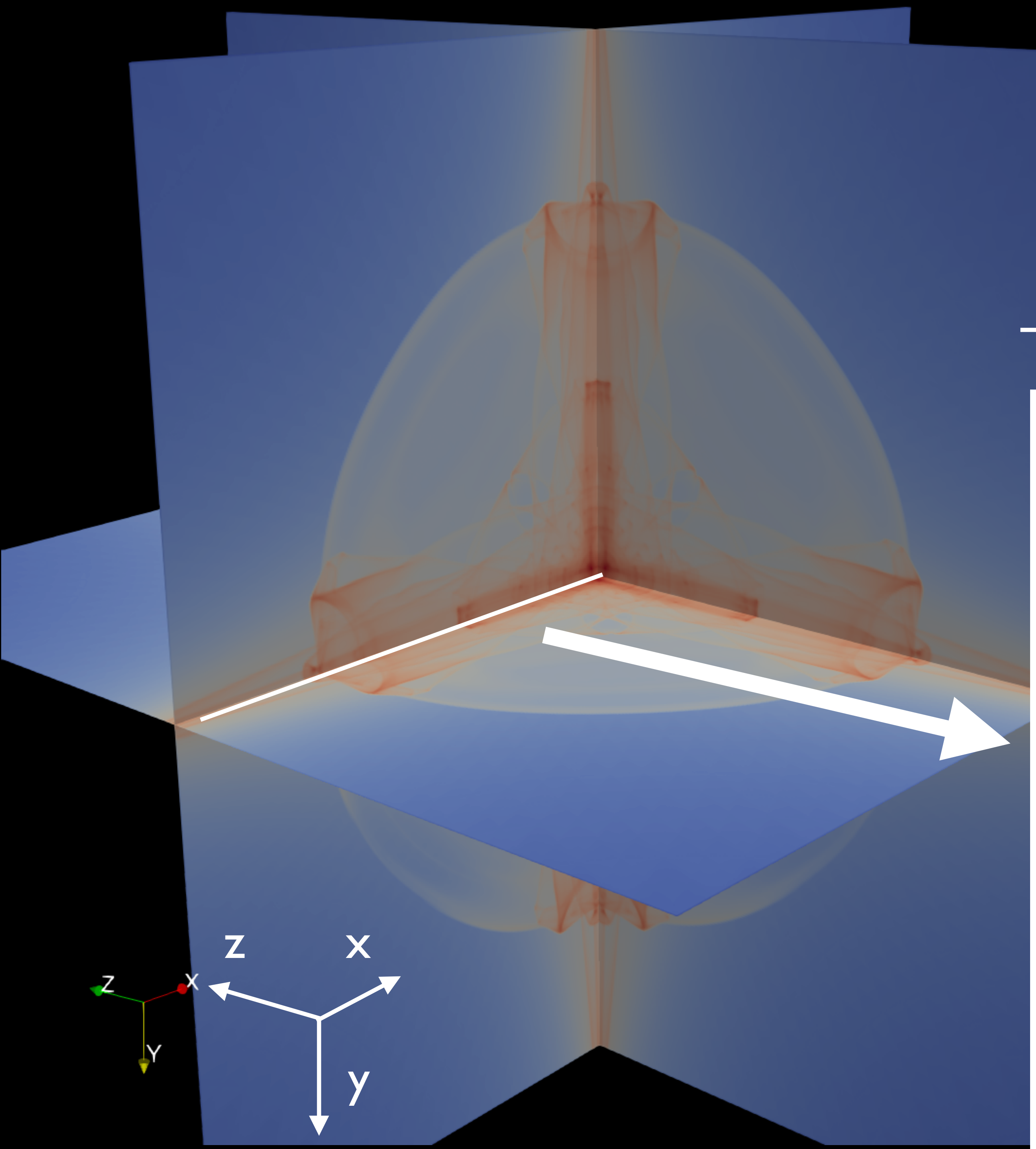

Single density peak in a periodic boundary box

(sinusoidal function)

→ Shell-crossing happens at origin

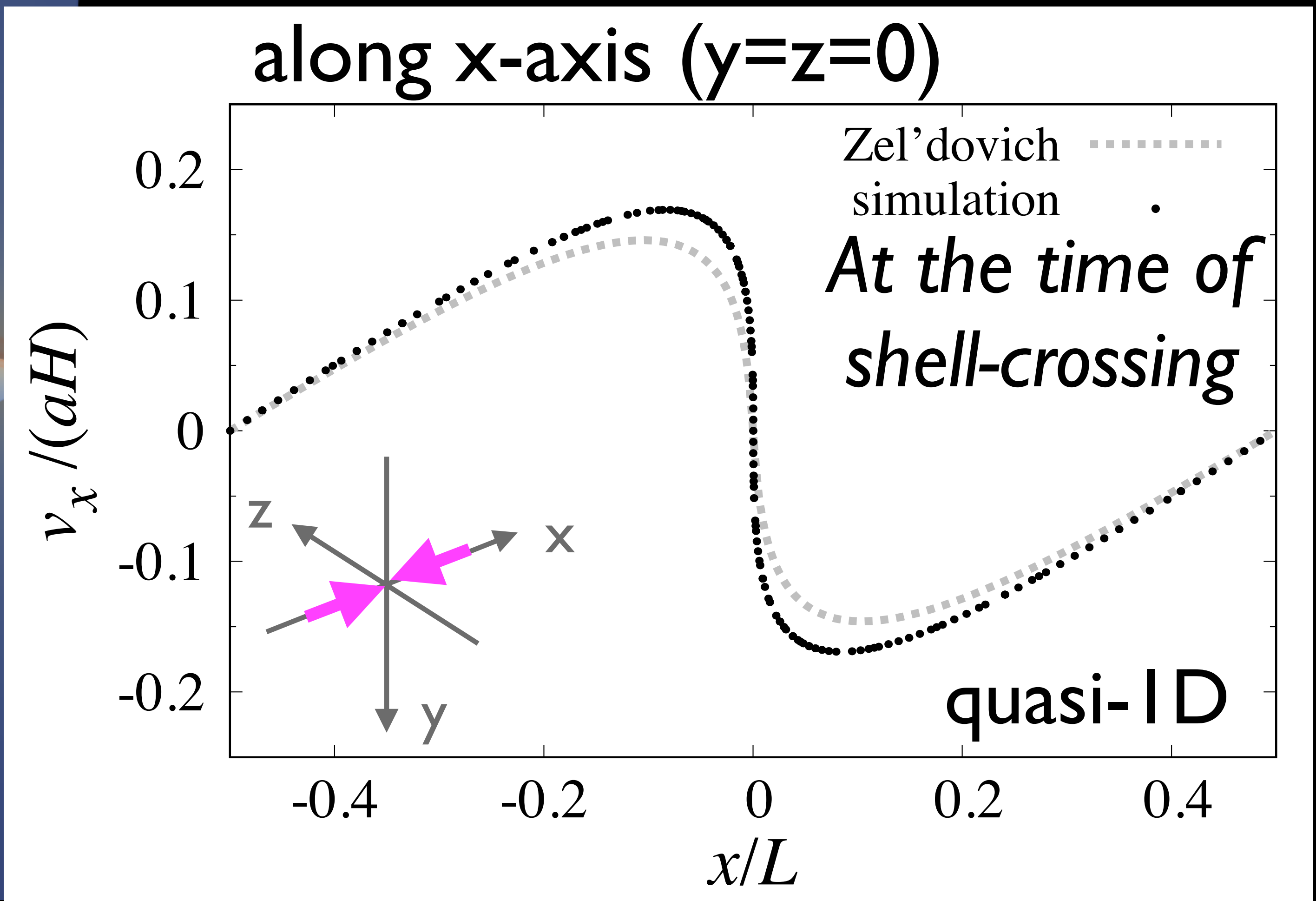

Vlasov simulation vs LPT

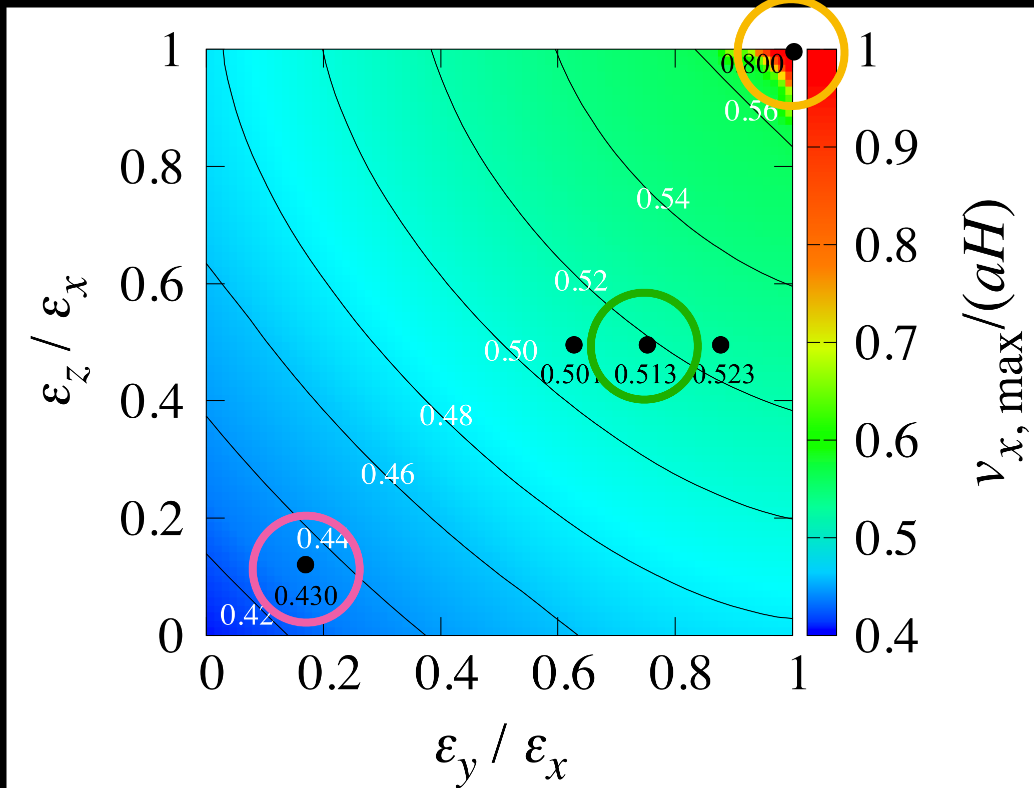

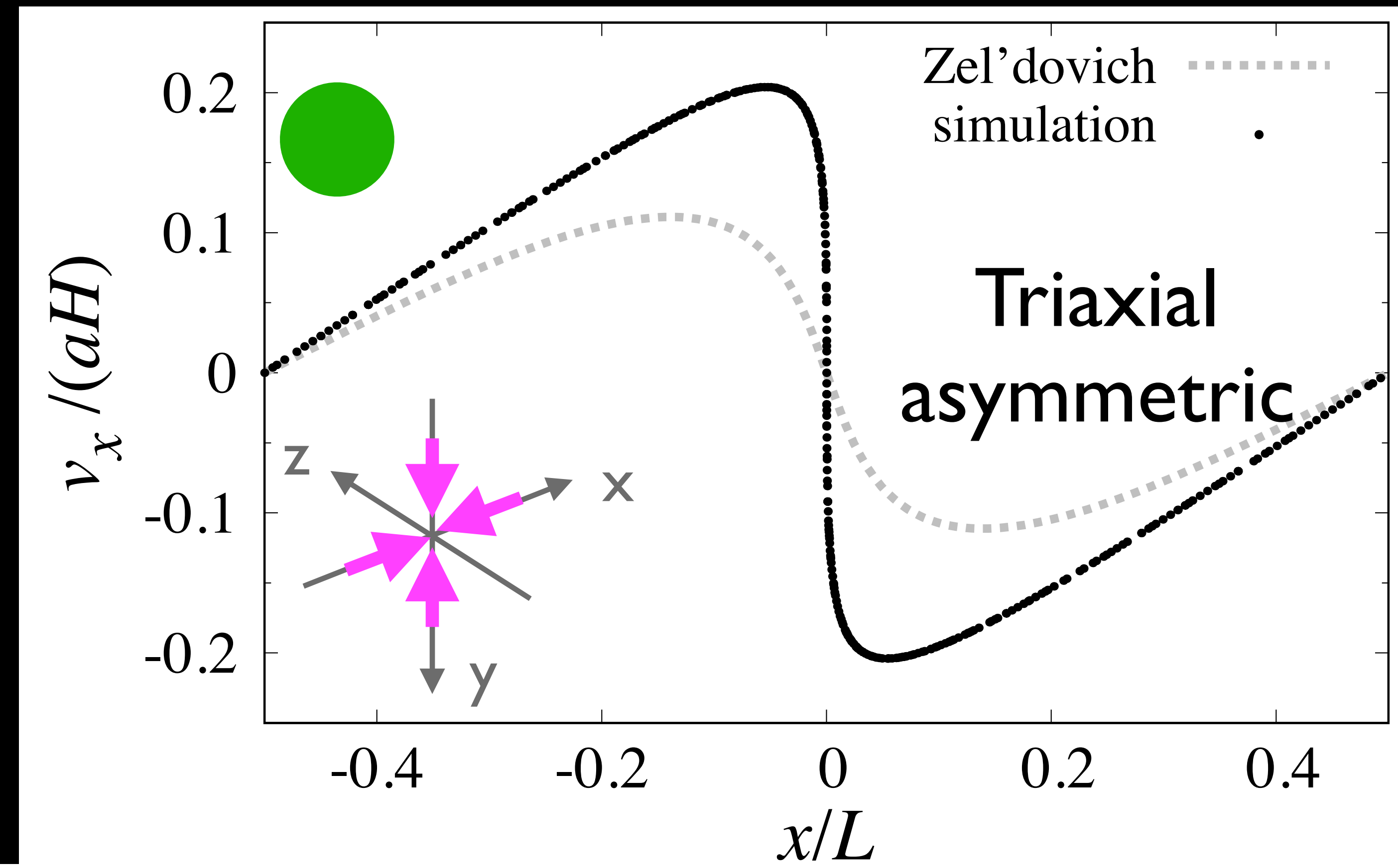

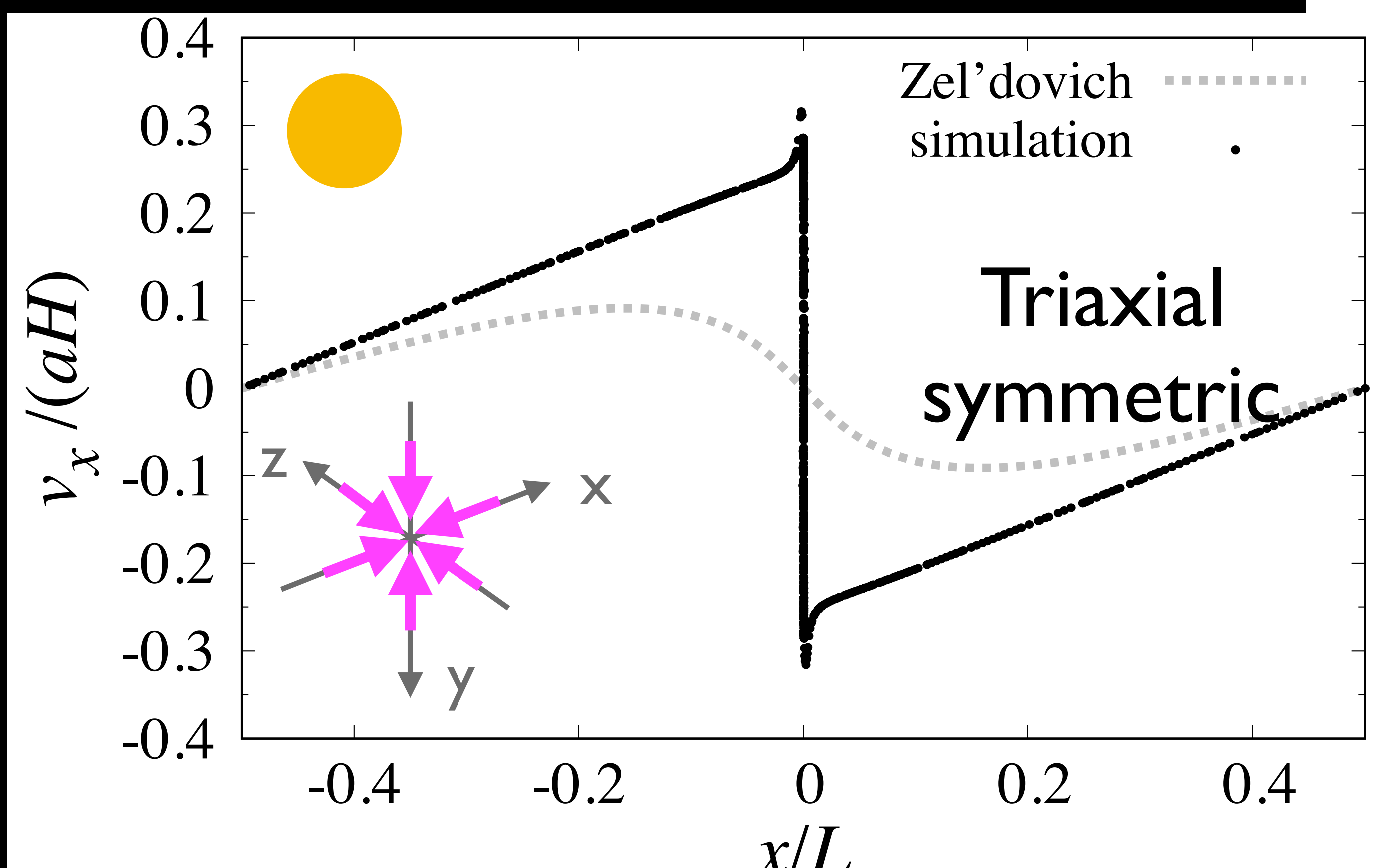

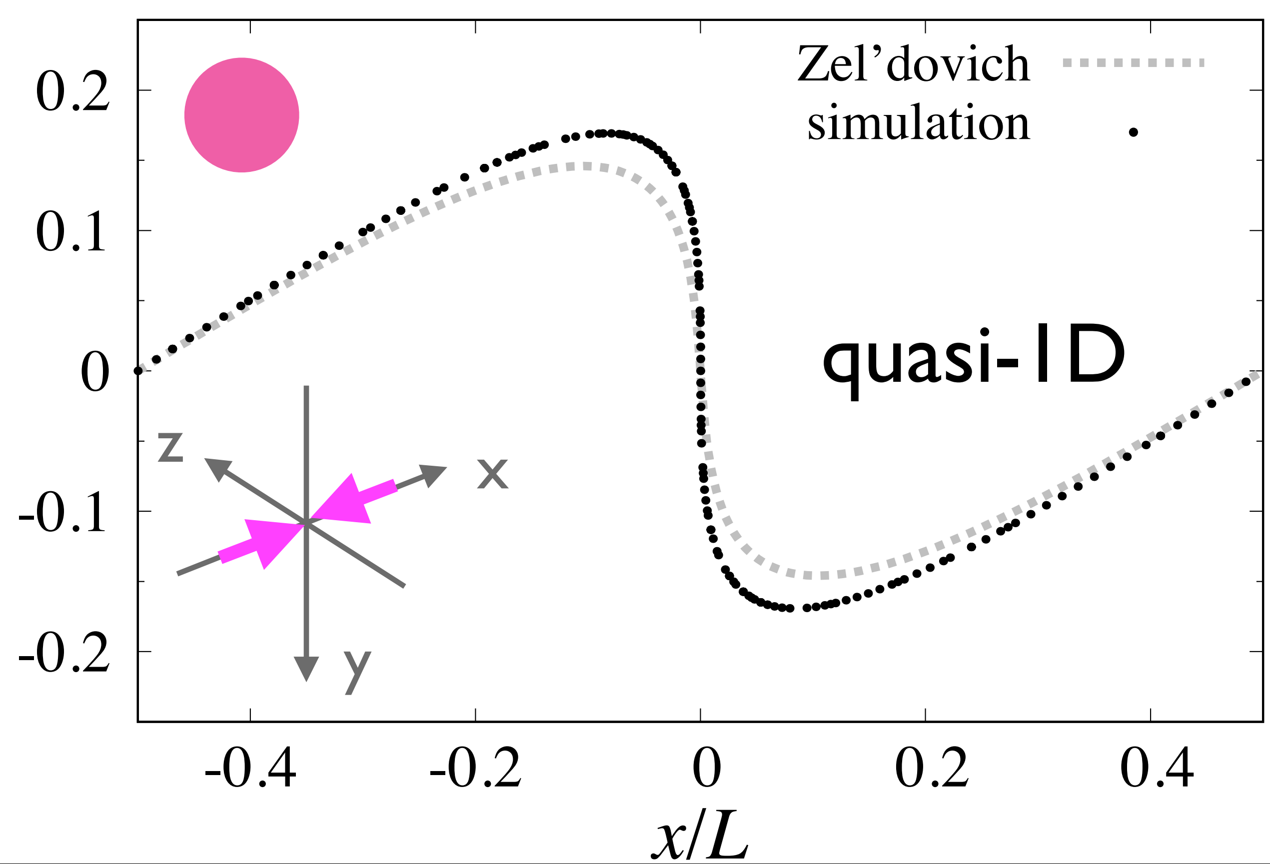

Vlasov simulation vs LPT

シェクルロッシング
時における比較

(原点で密度場発散)

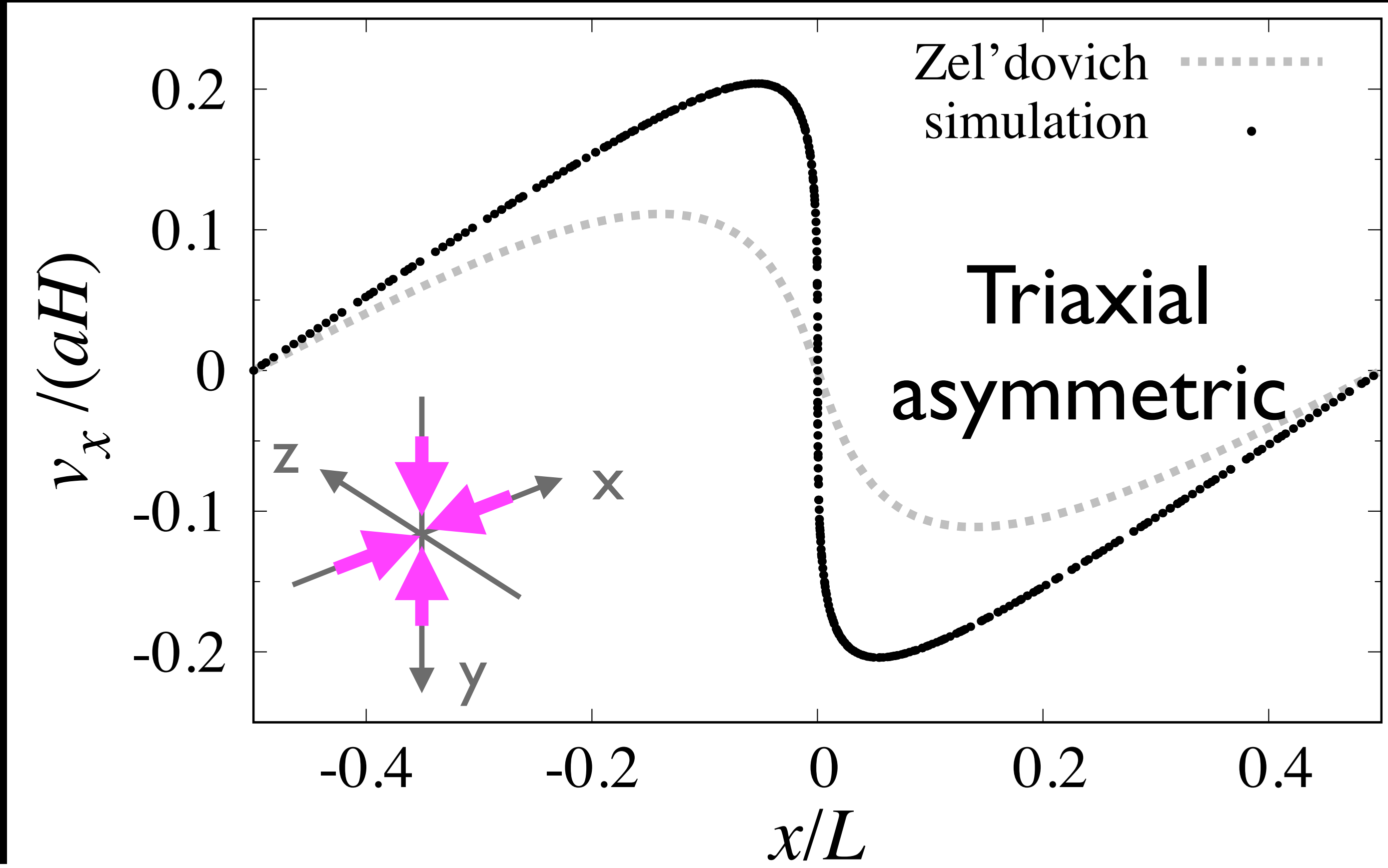

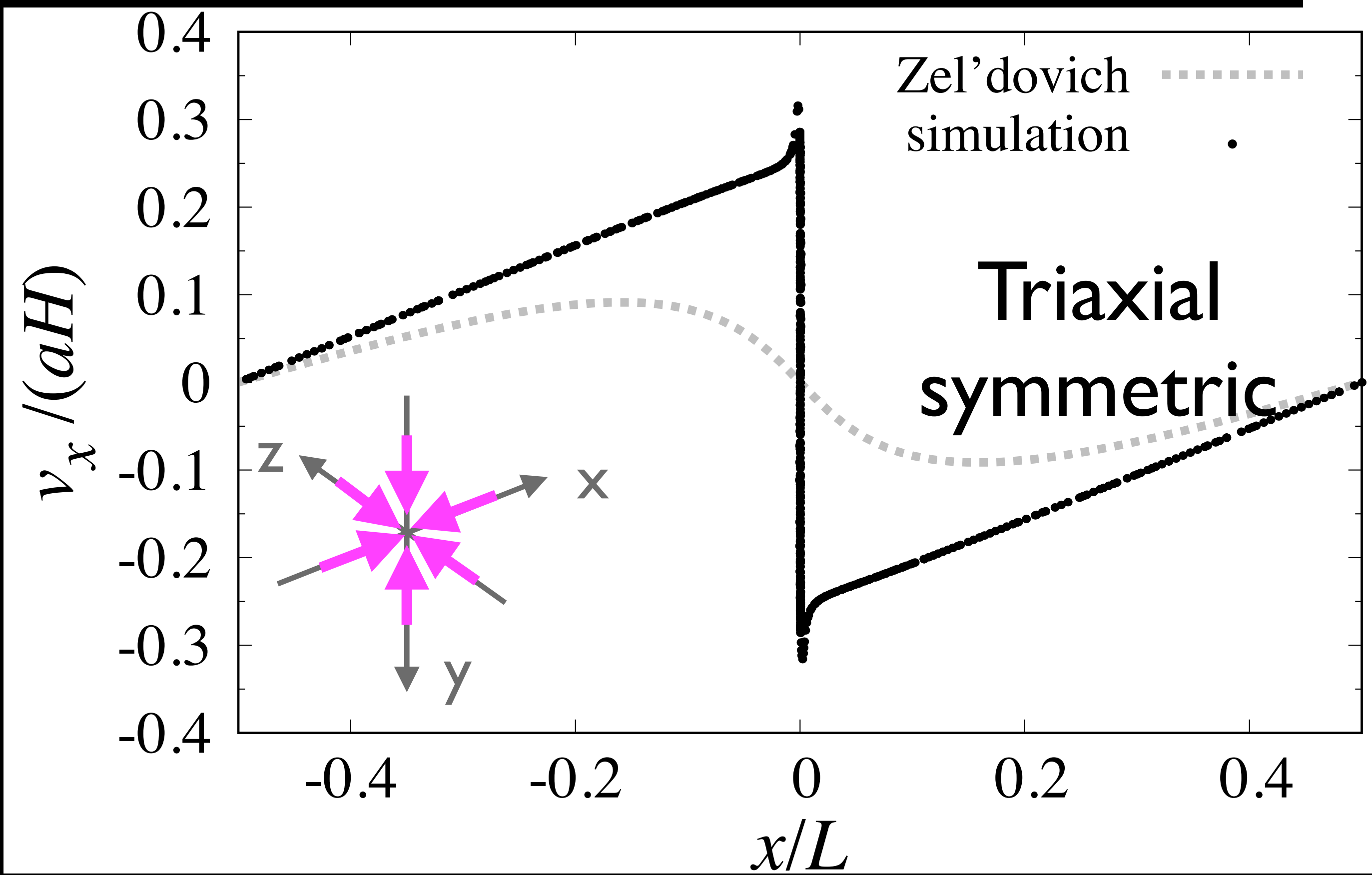

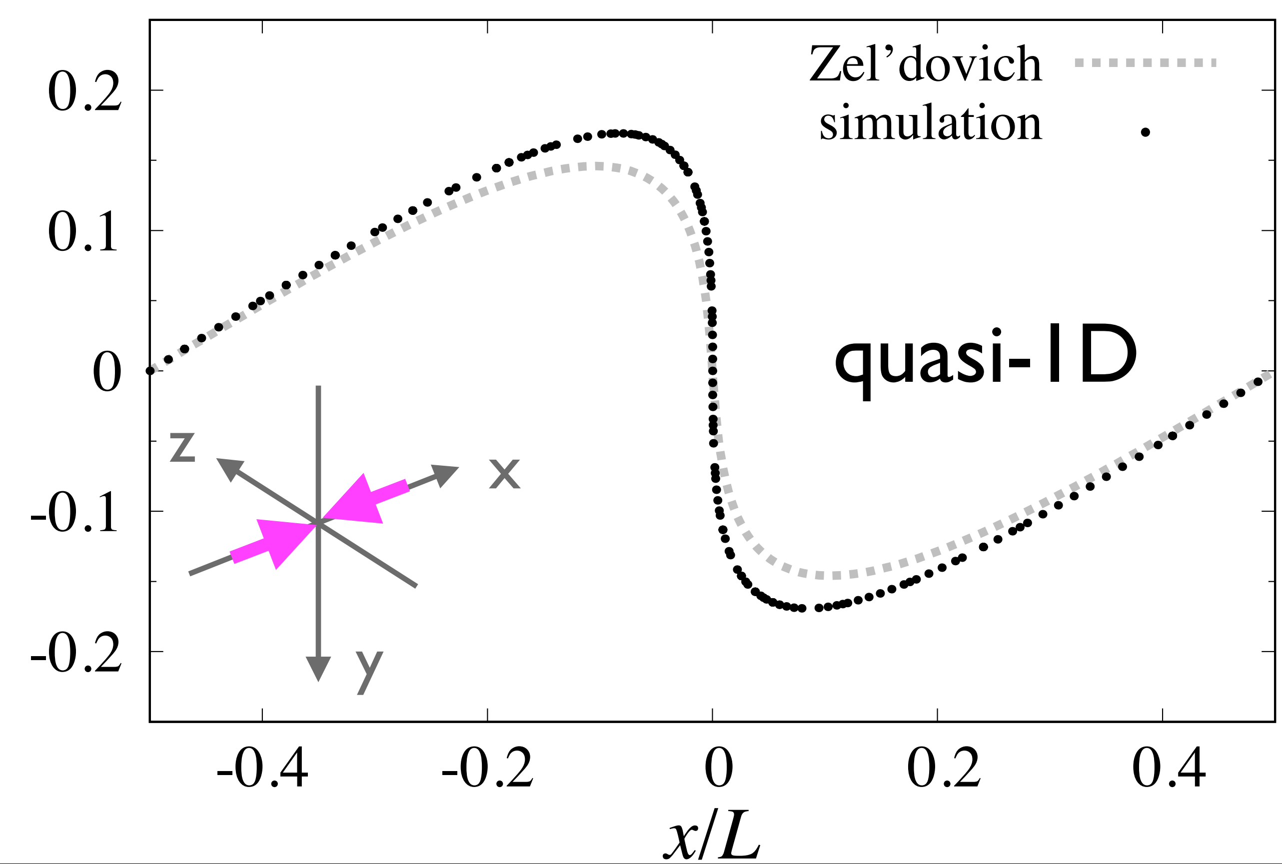

Vlasov simulation vs LPT

5th-order Lagrangian PT

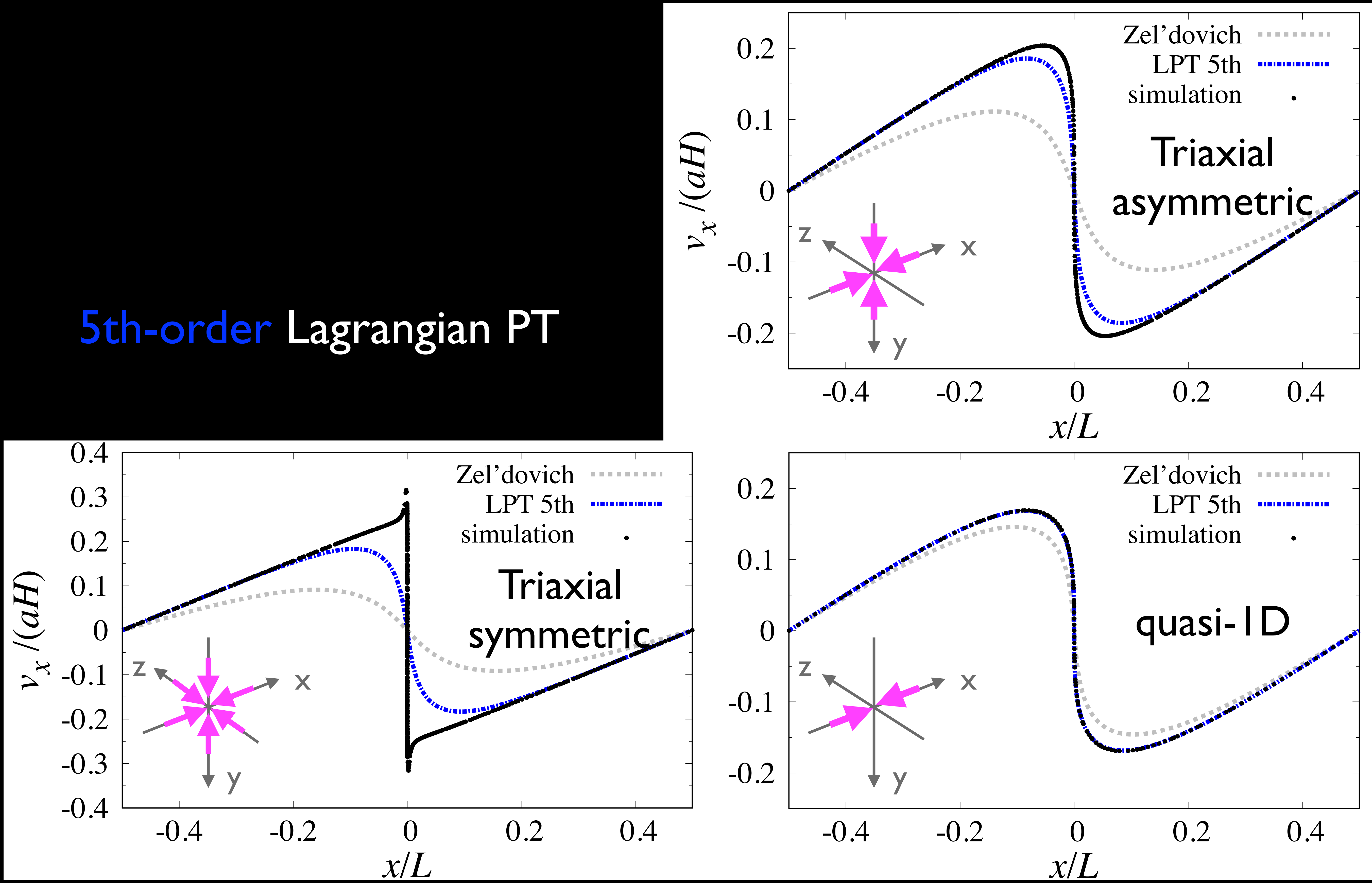

Vlasov simulation vs LPT

Making use of convergence of LPT expansion

$x_{\rm LPT}(\boldsymbol{q})$ at *n*-th order is found to be accurately fitted to

$$a + \frac{1}{b + c\,\exp[d\,n^{e}]} \quad \overset{n\to\infty}{\longrightarrow} \quad a$$

Extrapolation

$(a, \cdots, e: \text{ fitting parameter})$

at any Lagrangian position

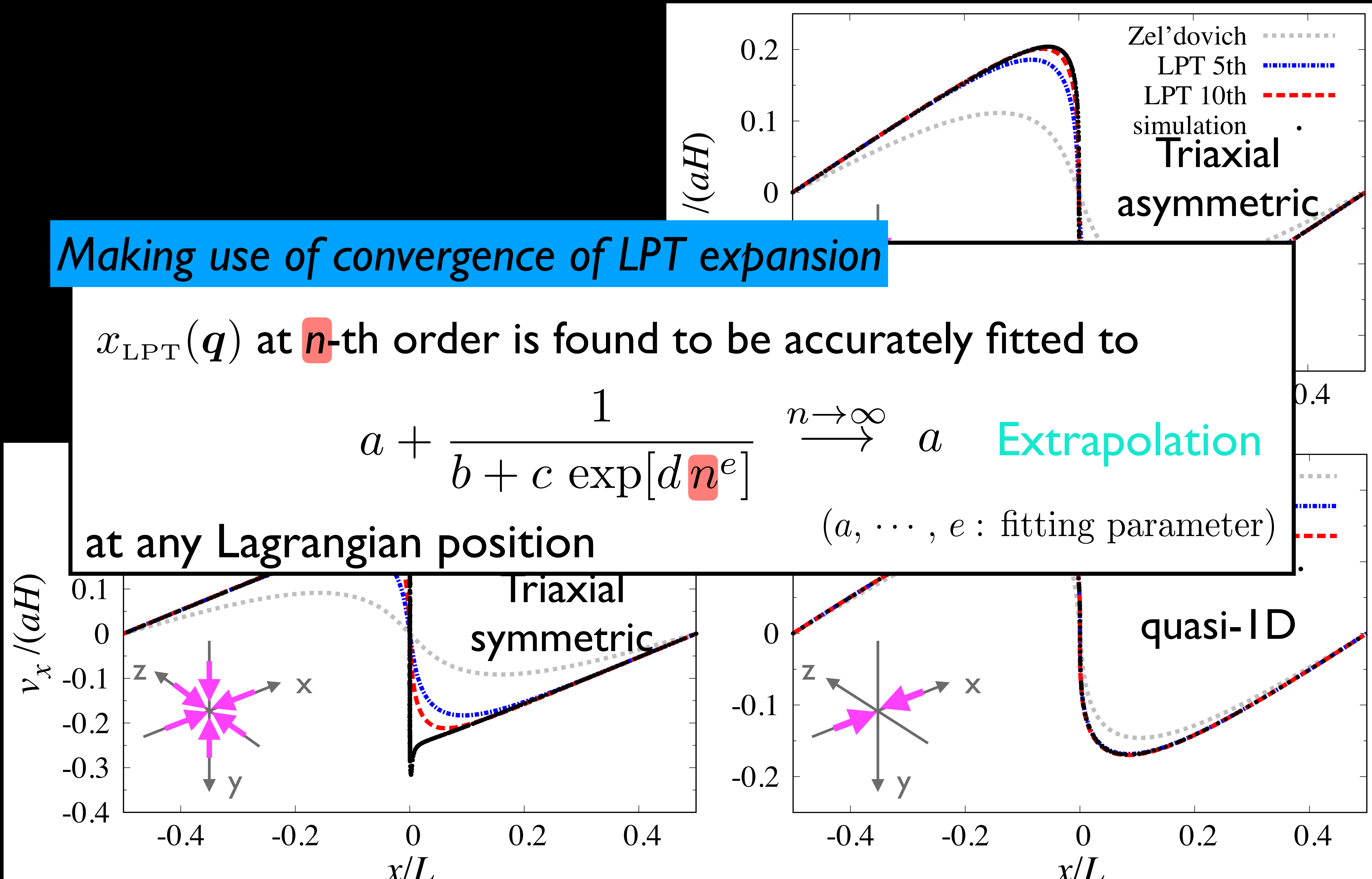

Vlasov simulation vs LPT

Extrapolation based on LPT

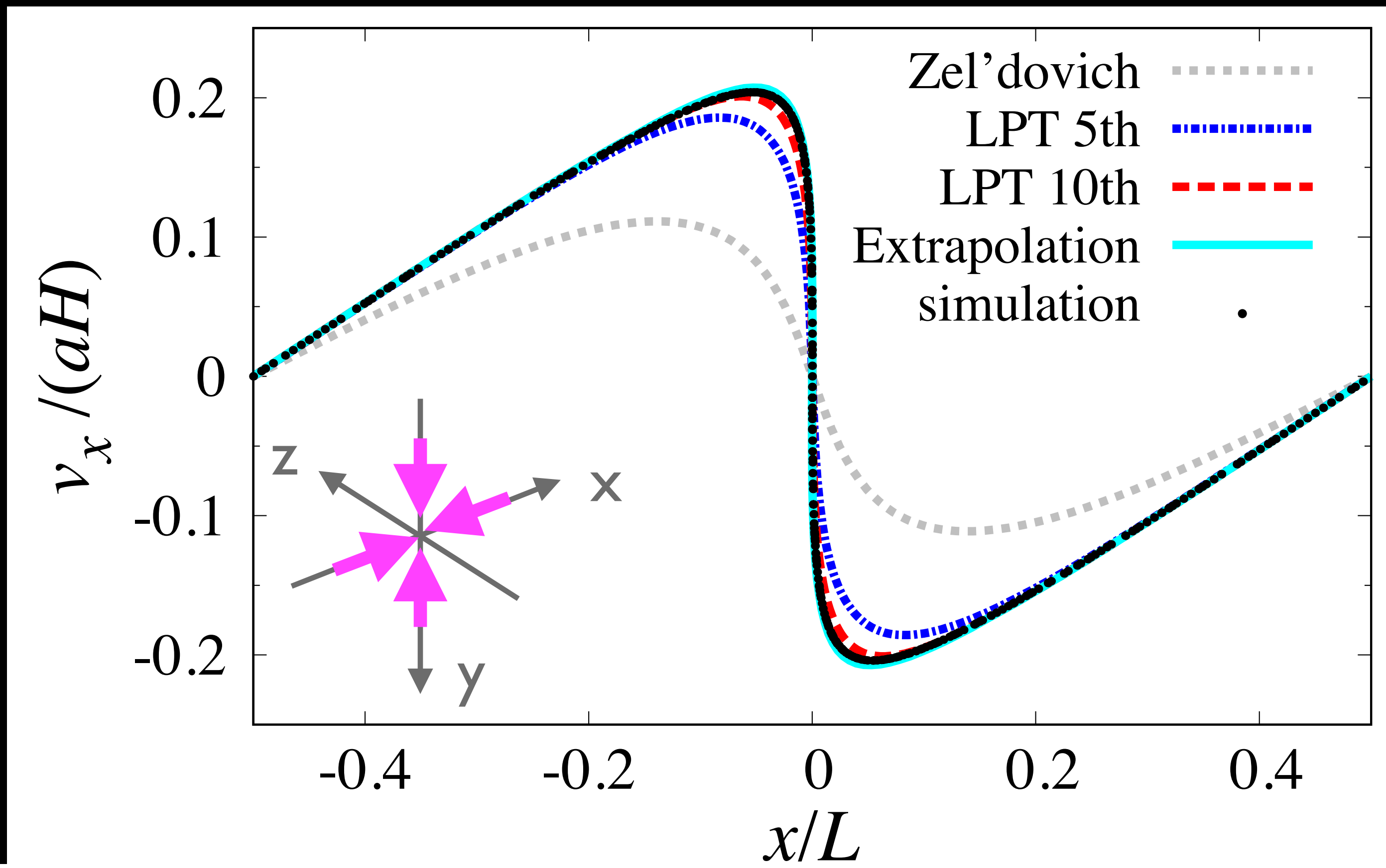

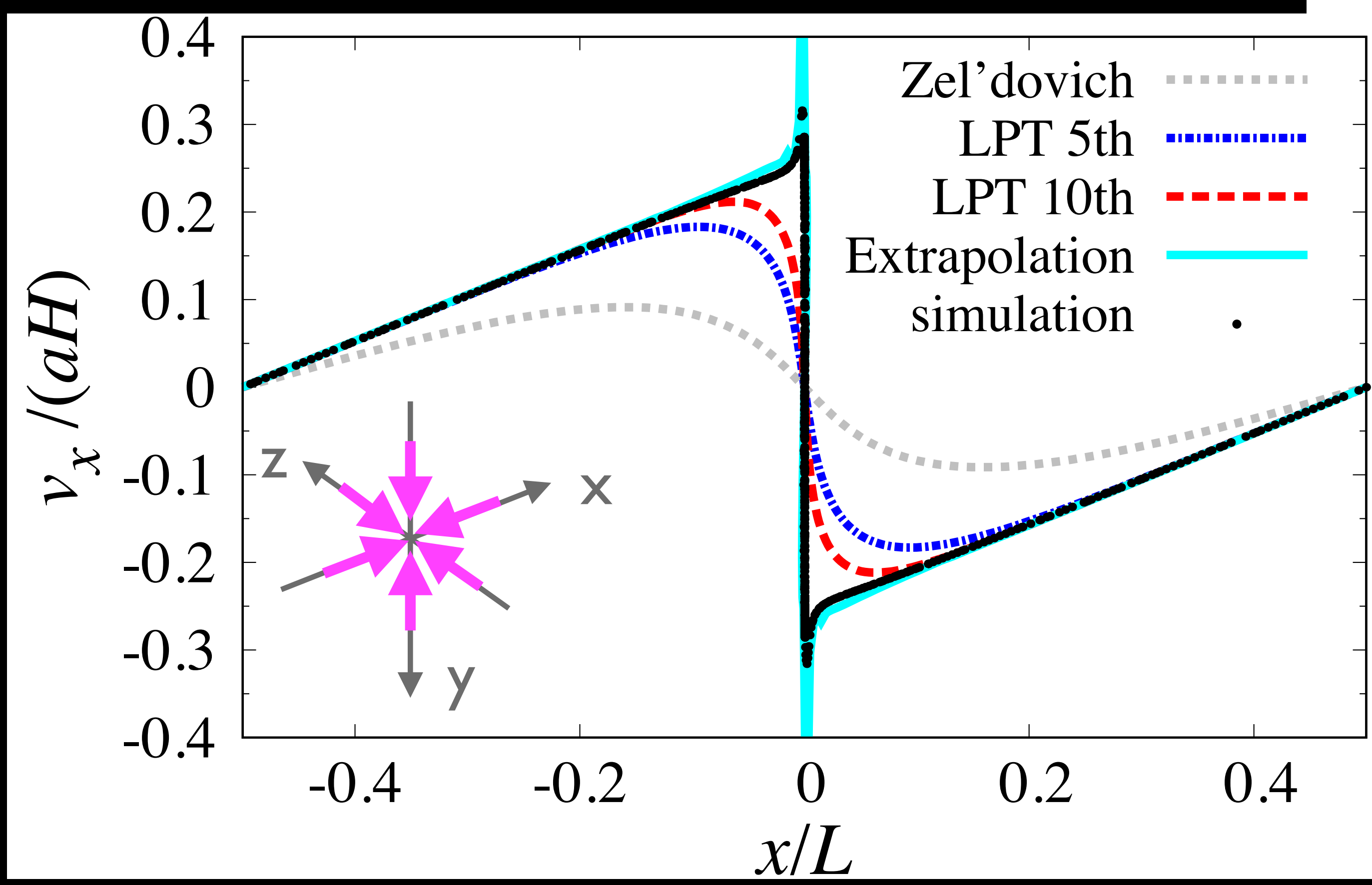

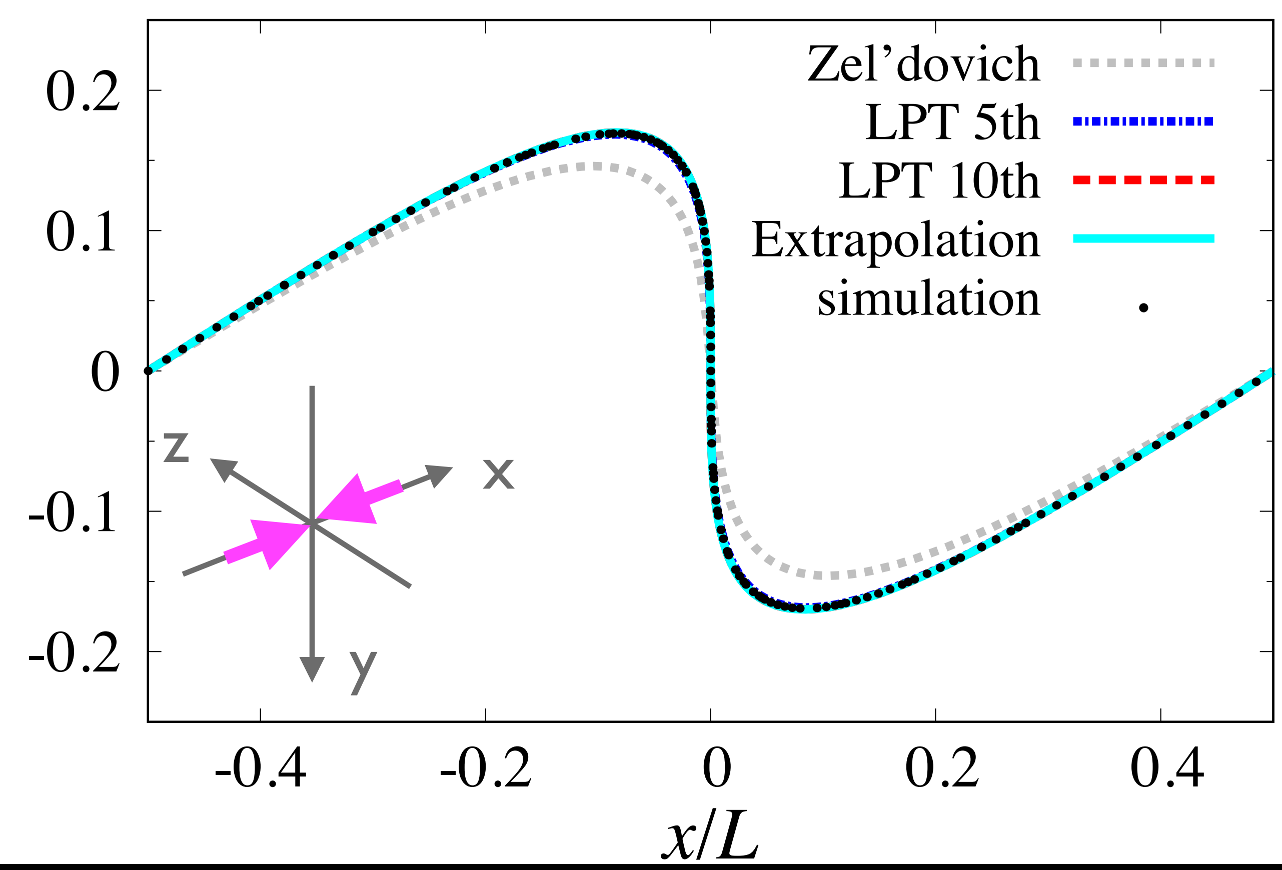

After shell-crossing,

quasi-1D collapse　　quasi-2D collapse　　3D collapse

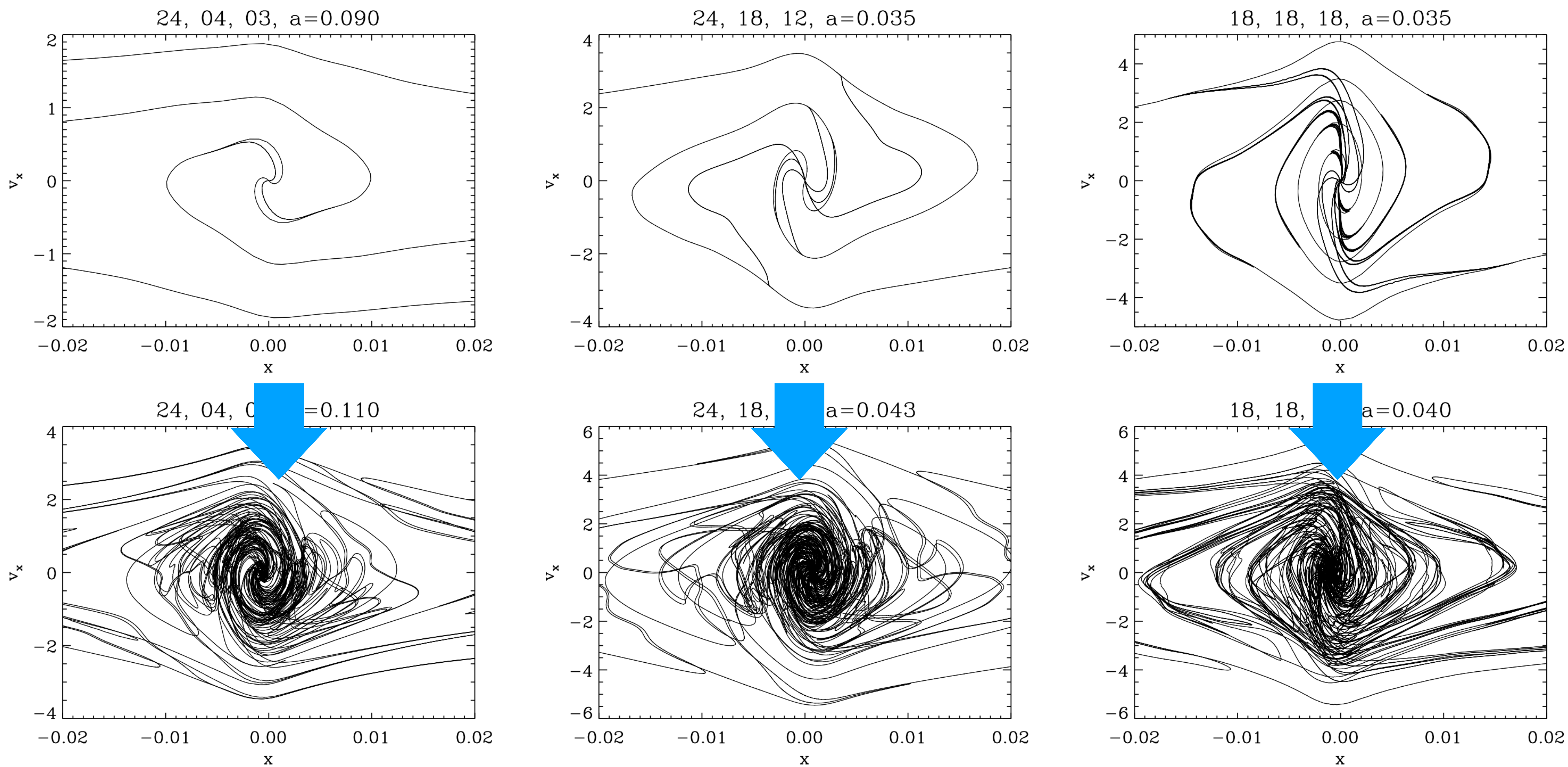

マルチストリーム構造が発達（ハローが形成）

Cosmological *N*-body simulations

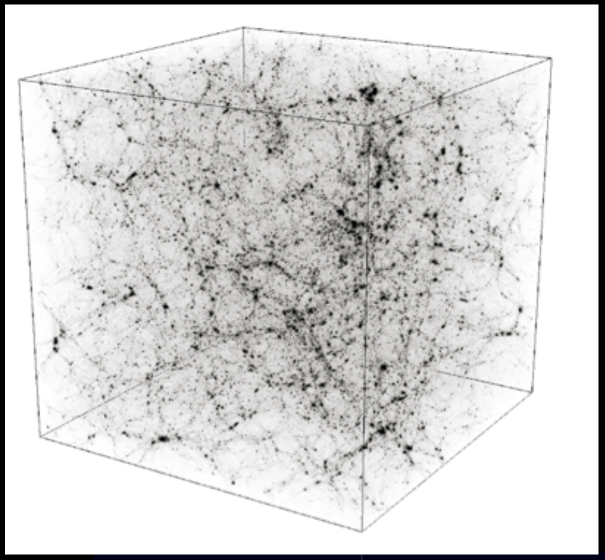

Directly solve equation of motion for *N* particles

→ Run *N*-body simulation many times with a large number of particles in a huge box

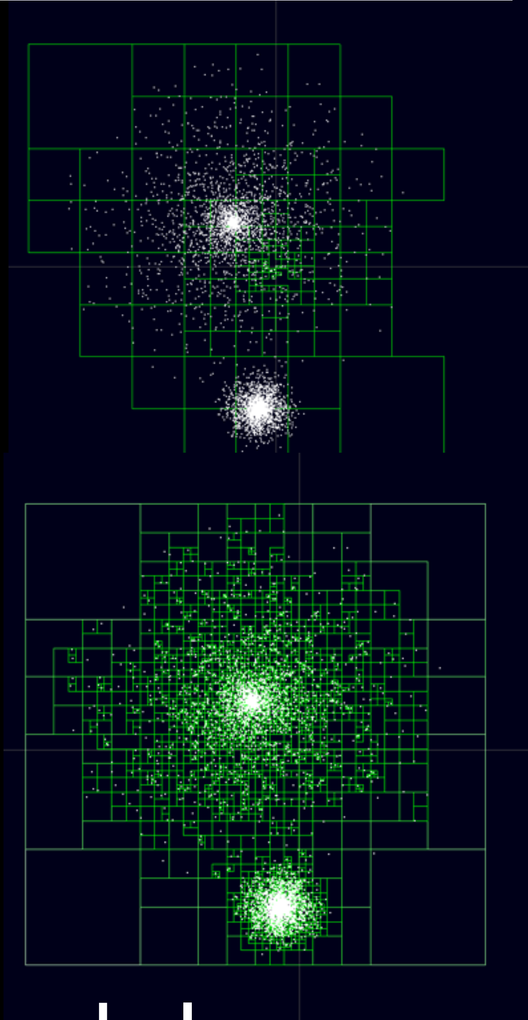

To reduce O(N^2) operation for force calculation,

O(N log N)
- Tree algorithm
- Particle-Mesh algorithm (using FFT)

For cosmological study

N~1,000^3, L~1,000 Mpc,   >50 runs

Still extensive but very useful for practical purposes :
mock data analysis, locating 'galaxies' in dark matter halo, …

Tree-PM method for force calculation

In Fourier space,

$$\phi_{\boldsymbol{k}} = \phi_{\boldsymbol{k}}^{\rm long} + \phi_{\boldsymbol{k}}^{\rm short}$$

$$\phi_{\boldsymbol{k}}^{\rm long} = \phi_{\boldsymbol{k}} \exp\left(-\boldsymbol{k}^2 r_{\rm s}^2 \right)$$

$$\phi_k^{\rm short} = \phi_k \left[1 - \exp(-\boldsymbol{k}^2 r_s^2)\right] \longrightarrow \phi^{\rm short}(\boldsymbol{x}) = -G \sum_i \frac{m_i}{r_i} \mathrm{erfc}\left(\frac{r_i}{2 r_{\rm s}} \right)$$

$$r_i = \min(|\boldsymbol{x} - \boldsymbol{r}_i - \boldsymbol{n}L|)$$

- long-range: PM method with FFT
- short-range: Tree algorithm (Barnes-Hut oct-tree)

http://arborjs.org/docs/barnes-hut

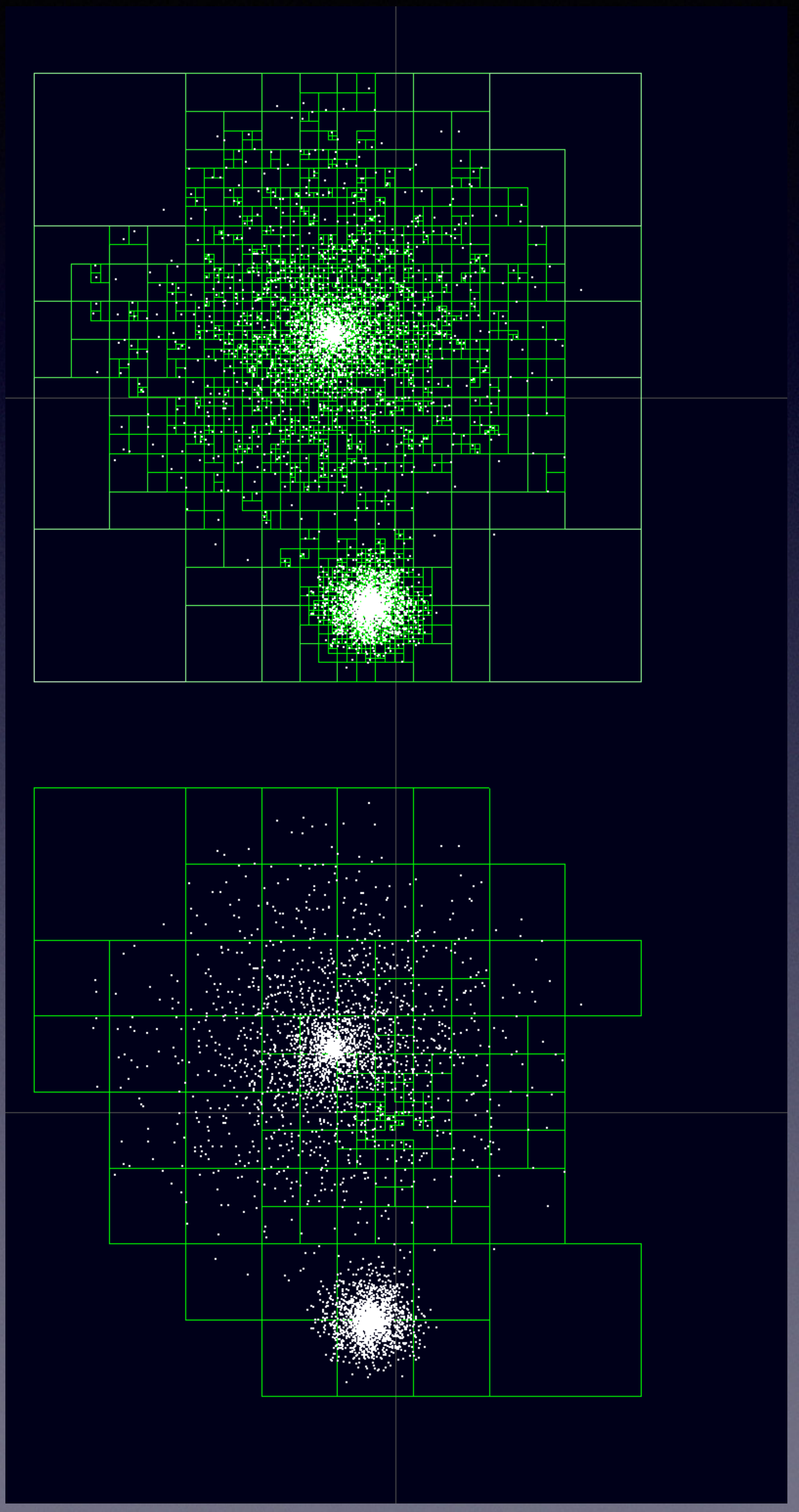

Performance of each method is O(N log N)

Cosmological initial condition

For particle assigned on each grid:

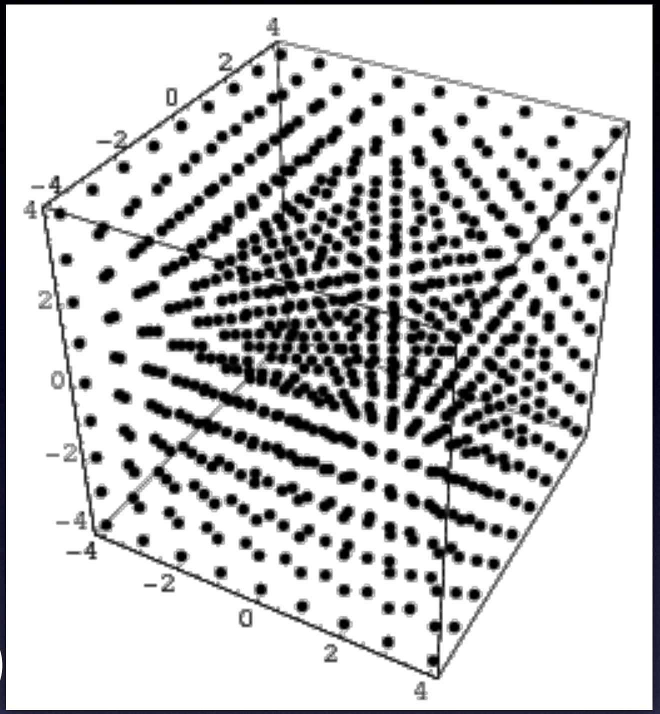

$$\boldsymbol{x} = \boldsymbol{q} + \boldsymbol{\Psi}(\boldsymbol{q})$$

initial position   Lagrangian displacement

Note $\boldsymbol{v} = a\dot{\boldsymbol{x}} = a\dot{\boldsymbol{\Psi}}(\boldsymbol{q})$

'q' is called Lagrangian coordinate (homogeneous mass dist)

leading order (Zel'dovich approx.)

$$\Psi(\boldsymbol{k}) \simeq \frac{i\,\boldsymbol{k}}{k^2} D_+(z) \delta_0(\boldsymbol{k})$$

initial density field (random)

General procedure

Improved initial condition generator with Lagrangian PT (2LPT code)

1. generate random field $\delta_0(\boldsymbol{k})$
2. calculate displacement field $\boldsymbol{\Psi}(\boldsymbol{k}) \xrightarrow{\text{FFT}} \boldsymbol{\Psi}(\boldsymbol{q})$
3. move particles according to displacement field $\boldsymbol{\Psi}(\boldsymbol{q})$ $\dot{\boldsymbol{\Psi}}(\boldsymbol{q}) = \frac{\dot{D}_+(z)}{D_+(z)} \boldsymbol{\Psi}(\boldsymbol{q})$

オイラー的摂動論

Perturbation theory (PT)

Theory of large-scale structure based on gravitational instability

Juszkiewicz ('81), Vishniac ('83), Goroff et al. ('86), Suto & Sasaki ('91), Jain & Bertschinger ('94), ...

Cold dark matter + baryons = pressureless & irrotational fluid

Basic eqs.

$$\frac{\partial \delta}{\partial t} + \frac{1}{a}\vec{\nabla}\cdot\left[(1+\delta)\vec{v}\right] = 0$$

$$\frac{\partial \vec{v}}{\partial t} + \frac{\dot{a}}{a}\vec{v} + \frac{1}{a}(\vec{v}\cdot\vec{\nabla})\vec{v} = -\frac{1}{a}\vec{\nabla}\Phi$$

$$\frac{1}{a^2}\nabla^2\Phi = 4\pi G\,\overline{\rho}_{\mathrm{m}}\,\delta$$

Single-stream approx. of collisionless Boltzmann eq.

standard PT
$|\delta| \ll 1$

$$\delta = \delta^{(1)} + \delta^{(2)} + \delta^{(3)} + \cdots \qquad \langle \delta(\boldsymbol{k};t)\delta(\boldsymbol{k}';t)\rangle = (2\pi)^3\,\delta_{\mathrm{D}}(\boldsymbol{k}+\boldsymbol{k}')\,P(|\boldsymbol{k}|;t)$$

Equations of motion

$$\partial_\tau \delta + \partial_i \left[(1+\delta) v^i \right] \; = \; 0 \; ,$$

$$\partial_\tau v^i + \mathcal{H} \, v_l^i + \partial^i \phi + v_l^j \, \partial_j v^i \;\; = 0$$

$$\triangle \, \phi \;\; = \;\; \frac{3}{2} \mathcal{H}^2 \Omega_m \, \delta \; .$$

τ: conformal time

(adτ = dt)

$$\int_{\boldsymbol{q}} \;\; \equiv \;\; \int \frac{d^3 \boldsymbol{q}}{(2\pi)^3}$$

Fourier expansion

$$\partial_\tau \delta(\boldsymbol{k}, \tau) + \theta(\boldsymbol{k}, \tau) \;\; = \;\; - \int_{\boldsymbol{q}} \alpha(\boldsymbol{q}, \boldsymbol{k} - \boldsymbol{q}) \, \theta(\boldsymbol{q}, \tau) \delta(\boldsymbol{k} - \boldsymbol{q}, \tau) \; ,$$

$$\partial_\tau \theta(\boldsymbol{k}, \tau) + \mathcal{H} \, \theta(\boldsymbol{k}, \tau) + \frac{3}{2} \Omega_m \mathcal{H}^2 \delta(\boldsymbol{k}, \tau)$$

$$= \;\; - \int_{\boldsymbol{q}} \beta(\boldsymbol{q}, \boldsymbol{k} - \boldsymbol{q}) \, \theta(\boldsymbol{q}, \tau) \theta(\boldsymbol{k} - \boldsymbol{q}, \tau)$$

$$\theta \equiv \nabla \cdot \boldsymbol{v}$$

$$\alpha(\boldsymbol{q}_1, \boldsymbol{q}_2) \;\; \equiv \;\; \frac{\boldsymbol{q}_1 \cdot (\boldsymbol{q}_1 + \boldsymbol{q}_2)}{q_1^2} \; , \qquad \beta(\boldsymbol{q}_1, \boldsymbol{q}_2) \;\; \equiv \;\; \frac{1}{2} \, (\boldsymbol{q}_1 + \boldsymbol{q}_2)^2 \, \frac{\boldsymbol{q}_1 \cdot \boldsymbol{q}_2}{q_1^2 \, q_2^2} \; .$$

Standard perturbation theory

$$\delta(\boldsymbol{k},a) = \sum_{i=1}^{\infty}\delta_{(i)}(\boldsymbol{k},a)\,, \qquad \theta(\boldsymbol{k},a) = -\mathcal{H}\,f(a)\sum_{i=1}^{\infty}\theta_{(i)}(\boldsymbol{k},a)$$

$$f(a) \equiv d\ln D_1/d\ln a$$

$D_1(a)$: Linear growth factor

Adopting the E-dS approximation,

$$\delta_{(n)}(\boldsymbol{k},a) = \underline{D_1^n(a)}\,\delta_n(\boldsymbol{k})\,, \qquad \theta_{(n)}(\boldsymbol{k},a) = \underline{D_1^n(a)}\,\theta_n(\boldsymbol{k})\,.$$

Linear density field (Gaussian)

$$\delta_n(\boldsymbol{k}) = \int_{\boldsymbol{q}_1}\cdots\int_{\boldsymbol{q}_n}(2\pi)^3\delta_D^{(3)}(\boldsymbol{k}-\boldsymbol{q}_1\ldots-\boldsymbol{q}_n)\,F_n(\boldsymbol{q}_1,\ldots,\boldsymbol{q}_n)\,\delta_0(\boldsymbol{q}_1)\ldots\delta_0(\boldsymbol{q}_n)\,,$$

$$\theta_n(\boldsymbol{k}) = \int_{\boldsymbol{q}_1}\cdots\int_{\boldsymbol{q}_n}(2\pi)^3\delta_D^{(3)}(\boldsymbol{k}-\boldsymbol{q}_1\ldots-\boldsymbol{q}_n)\,G_n(\boldsymbol{q}_1,\ldots,\boldsymbol{q}_n)\,\delta_0(\boldsymbol{q}_1)\ldots\delta_0(\boldsymbol{q}_n)\,,$$

standard PT kernel $(F_1 = G_1 = 1)$

Recursion relation for PT kernels

$$\mathcal{F}_a^{(n)}(\boldsymbol{k}_1,\cdots,\boldsymbol{k}_n) \equiv \left[\begin{array}{c} F_n(\boldsymbol{k}_1,\cdots,\boldsymbol{k}_n) \\ G_n(\boldsymbol{k}_1,\cdots,\boldsymbol{k}_n) \end{array}\right]$$

$$\mathcal{F}_a^{(n)}(\boldsymbol{k}_1,\cdots,\boldsymbol{k}_n) = \sum_{m=1}^{n-1} \sigma_{ab}^{(n)}\,\gamma_{bcd}(\boldsymbol{q}_1,\boldsymbol{q}_2)\,\mathcal{F}_c^{(m)}(\boldsymbol{k}_1,\cdots,\boldsymbol{k}_m)\,\mathcal{F}_d^{(n-m)}(\boldsymbol{k}_{m+1},\cdots,\boldsymbol{k}_n)$$

$$\boldsymbol{q}_1 = \boldsymbol{k}_1 + \cdots + \boldsymbol{k}_m$$
$$\boldsymbol{q}_2 = \boldsymbol{k}_{m+1} + \cdots + \boldsymbol{k}_n$$

$$\sigma_{ab}^{(n)} = \frac{1}{(2n+3)(n-1)} \left(\begin{array}{cc} 2n+1 & 2 \\ 3 & 2n \end{array}\right)$$

$$\gamma_{abc}(\boldsymbol{k}_1,\boldsymbol{k}_2) = \begin{cases} \frac{1}{2}\left\{1+\frac{\boldsymbol{k}_2\cdot\boldsymbol{k}_1}{|\boldsymbol{k}_2|^2}\right\}; & (a,\,b,\,c)=(1,\,1,\,2) \\ \frac{1}{2}\left\{1+\frac{\boldsymbol{k}_1\cdot\boldsymbol{k}_2}{|\boldsymbol{k}_1|^2}\right\}; & (a,\,b,\,c)=(1,\,2,\,1) \\ \frac{(\boldsymbol{k}_1\cdot\boldsymbol{k}_2)|\boldsymbol{k}_1+\boldsymbol{k}_2|^2}{2|\boldsymbol{k}_1|^2|\boldsymbol{k}_2|^2}; & (a,\,b,\,c)=(2,\,2,\,2) \\ 0; & \text{otherwise.} \end{cases}$$

Note—. repetition of the same subscripts (a,b,c) indicates the sum over all multiplet components

PT kernels constructed from recursion relation should be symmetrized

Power spectrum

$$\langle \delta(\boldsymbol{k}_1, a)\delta(\boldsymbol{k}_2, a)\rangle \equiv (2\pi)^3 \delta_D^{(3)}(\boldsymbol{k}_1 + \boldsymbol{k}_2)\, P(k_1, a)$$

$$P_{SPT}(k) \;=\; \underbrace{P_{lin}(k)}_{\text{linear}} + \underbrace{P_{22}(k) + P_{13}(k)}_{\text{1-loop}} + \;\text{higher order loops}\;.$$

$$P_{22}(k) \;=\; 2\int_{\boldsymbol{q}} P_{lin}(q) P_{lin}(|\boldsymbol{k}-\boldsymbol{q}|)\, F_2^2(\boldsymbol{q}, \boldsymbol{k}-\boldsymbol{q})\;,$$

$$P_{13}(k) \;=\; 6 P_{lin}(k) \int_{\boldsymbol{q}} P_{lin}(q)\, F_3(\boldsymbol{k}, \boldsymbol{q}, -\boldsymbol{q})\;,$$

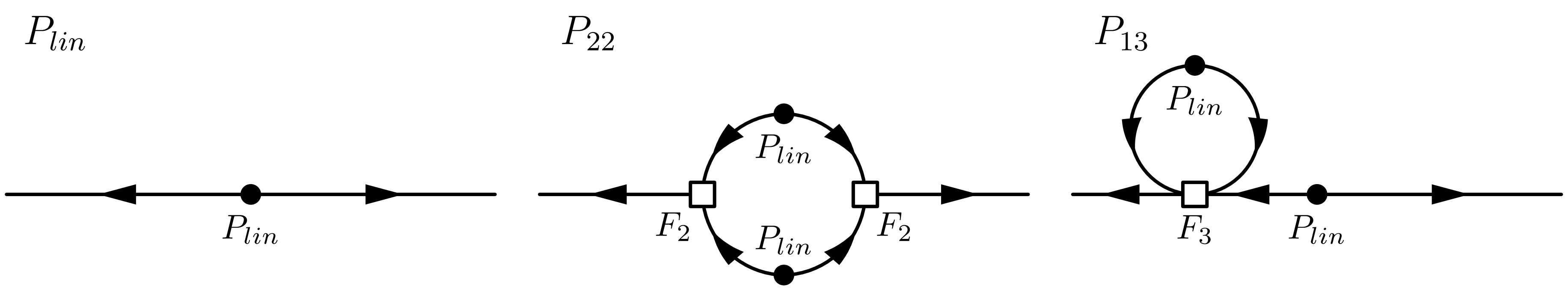

Next-to-next-to leading order

up to 2-loop order

$$P^{(mn)} \simeq \langle \delta^{(m)} \delta^{(n)} \rangle$$

$$P(k) = \underbrace{P^{(11)}(k)}_{\text{Linear (tree)}} + \underbrace{\left(P^{(22)}(k) + P^{(13)}(k)\right)}_{\text{1-loop}} + \underbrace{\left(P^{(33)}(k) + P^{(24)}(k) + P^{(15)}(k)\right)}_{\text{2-loop}} + \cdots$$

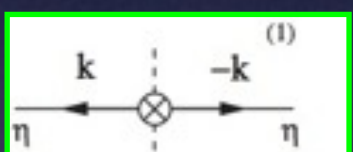

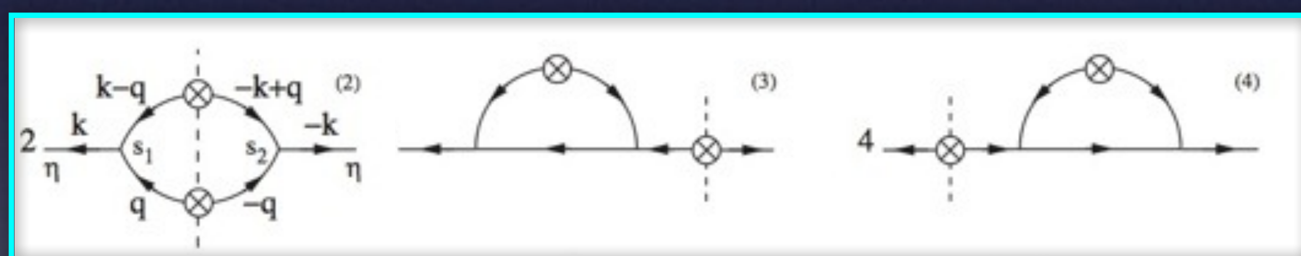

Crocce & Scoccimarro ('06)

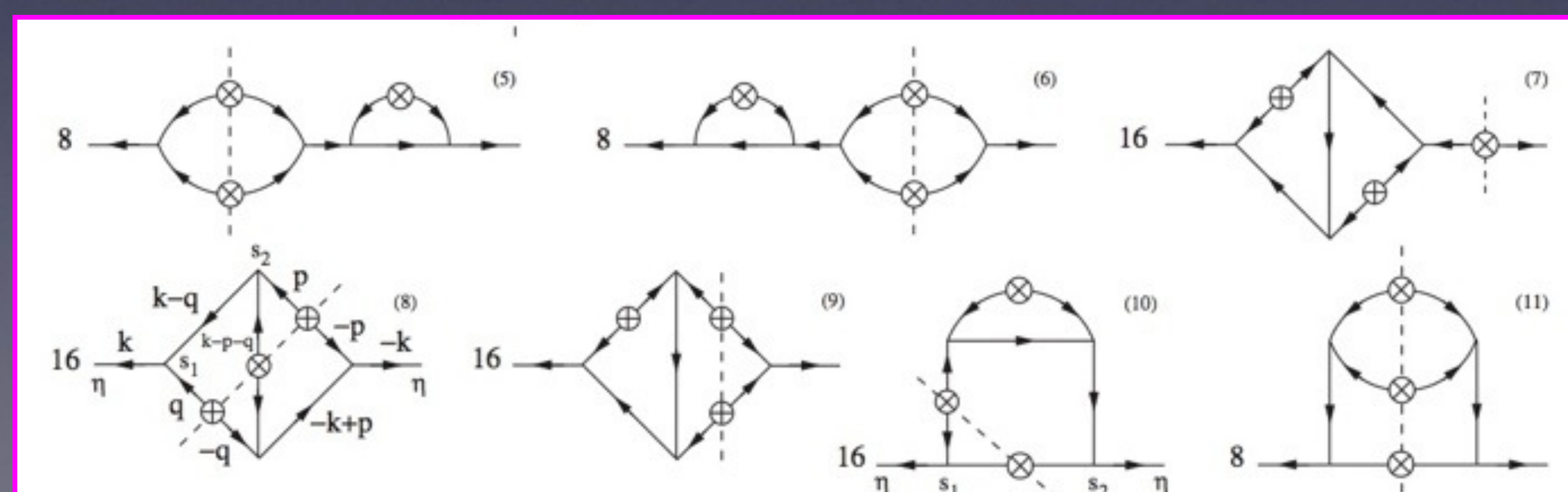

Calculation involves multi-dimensional numerical integration

(time-consuming)

Comparison with simulations

Standard PT qualitatively explains scale-dependent nonlinear growth, however,

1-loop :
overestimates simulations

2-loop :
overestimates at high-z, while it turn to underestimate at low-z

Standard PT produces ill-behaved PT expansion !!

… need to be improved

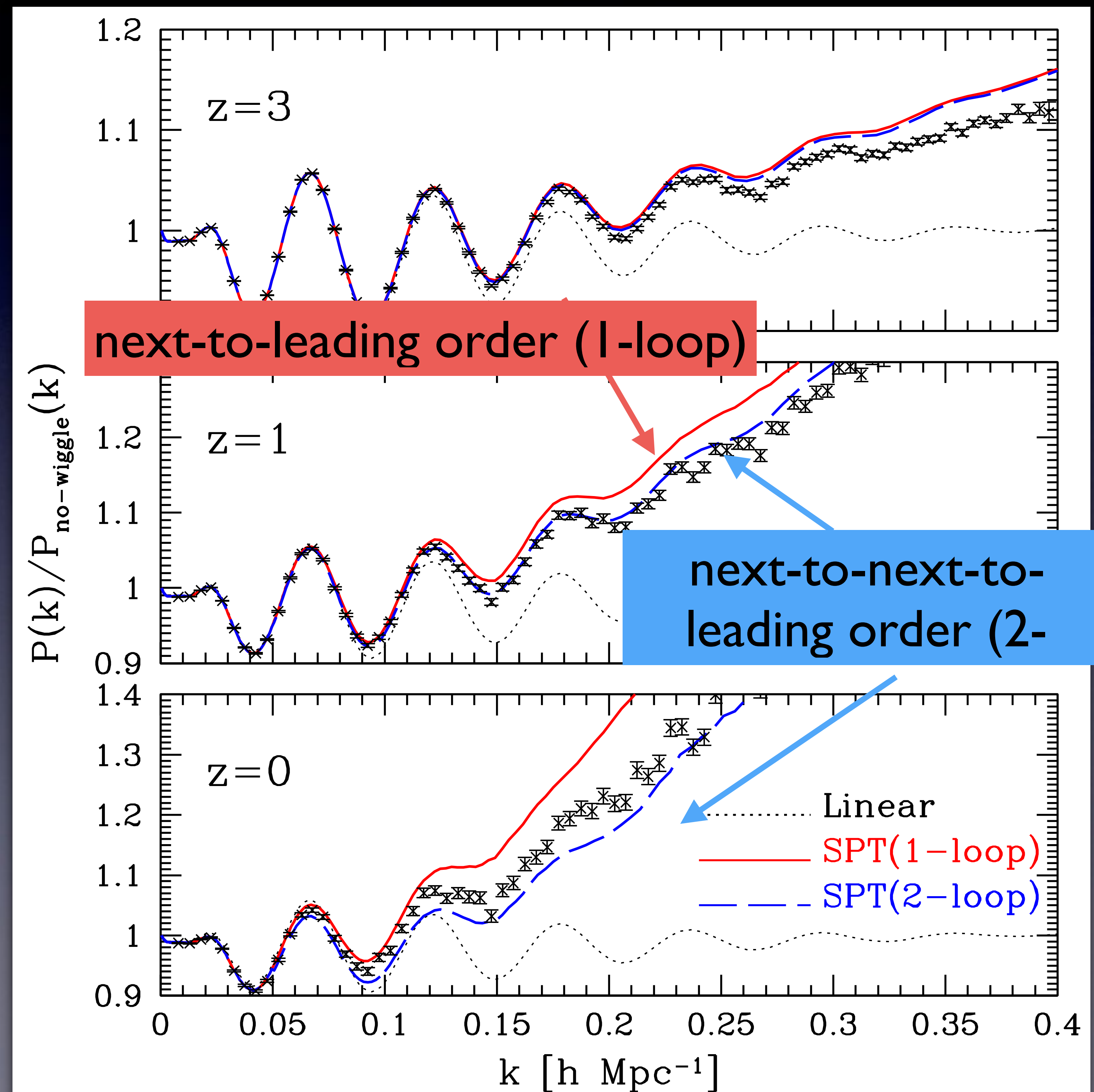

AT et al. ('09)

Density field in standard PT

Gaussian smoothing (10Mpc/h)

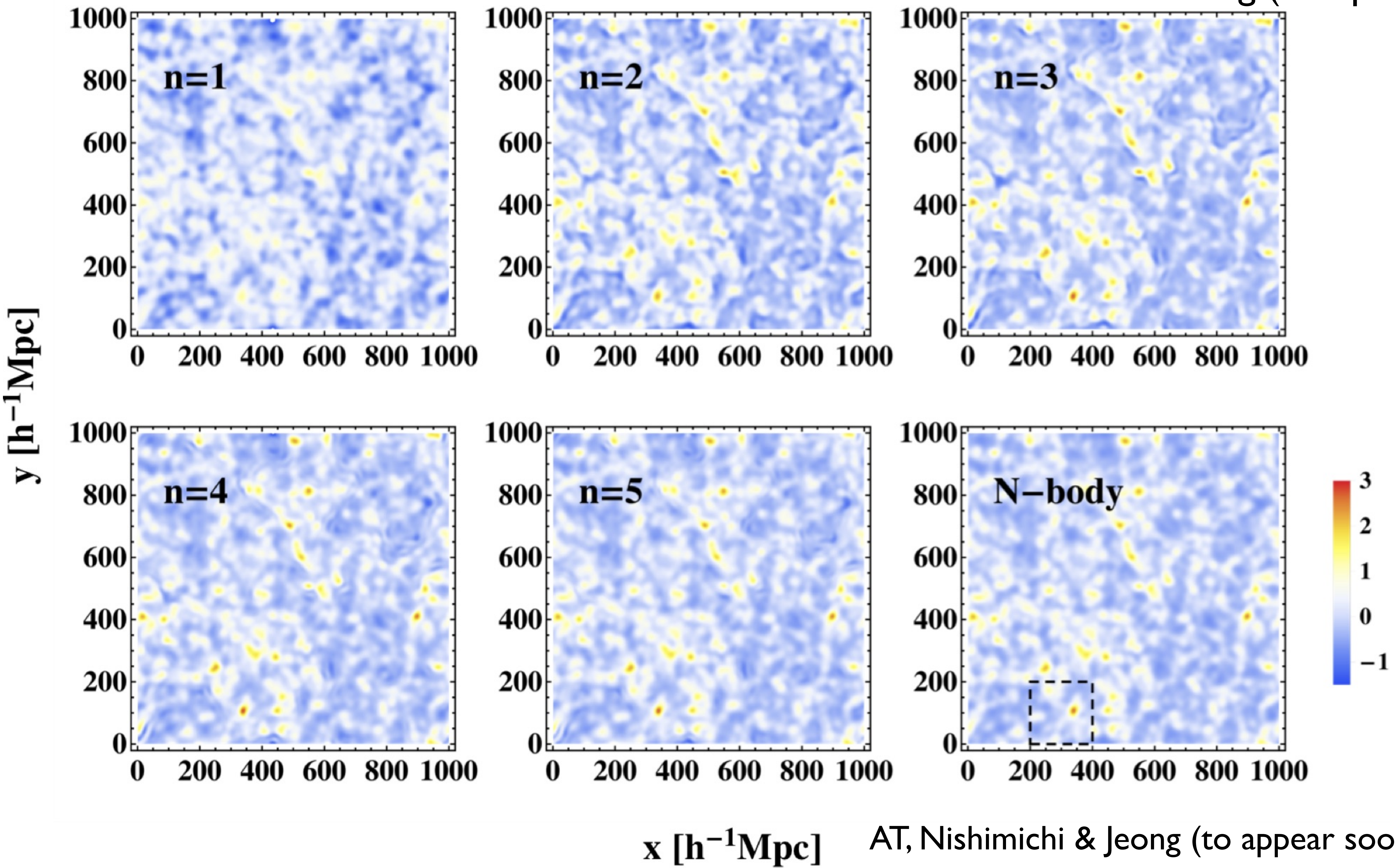

AT, Nishimichi & Jeong (to appear soon)

Density field in standard PT

Gaussian smoothing (10Mpc/h)

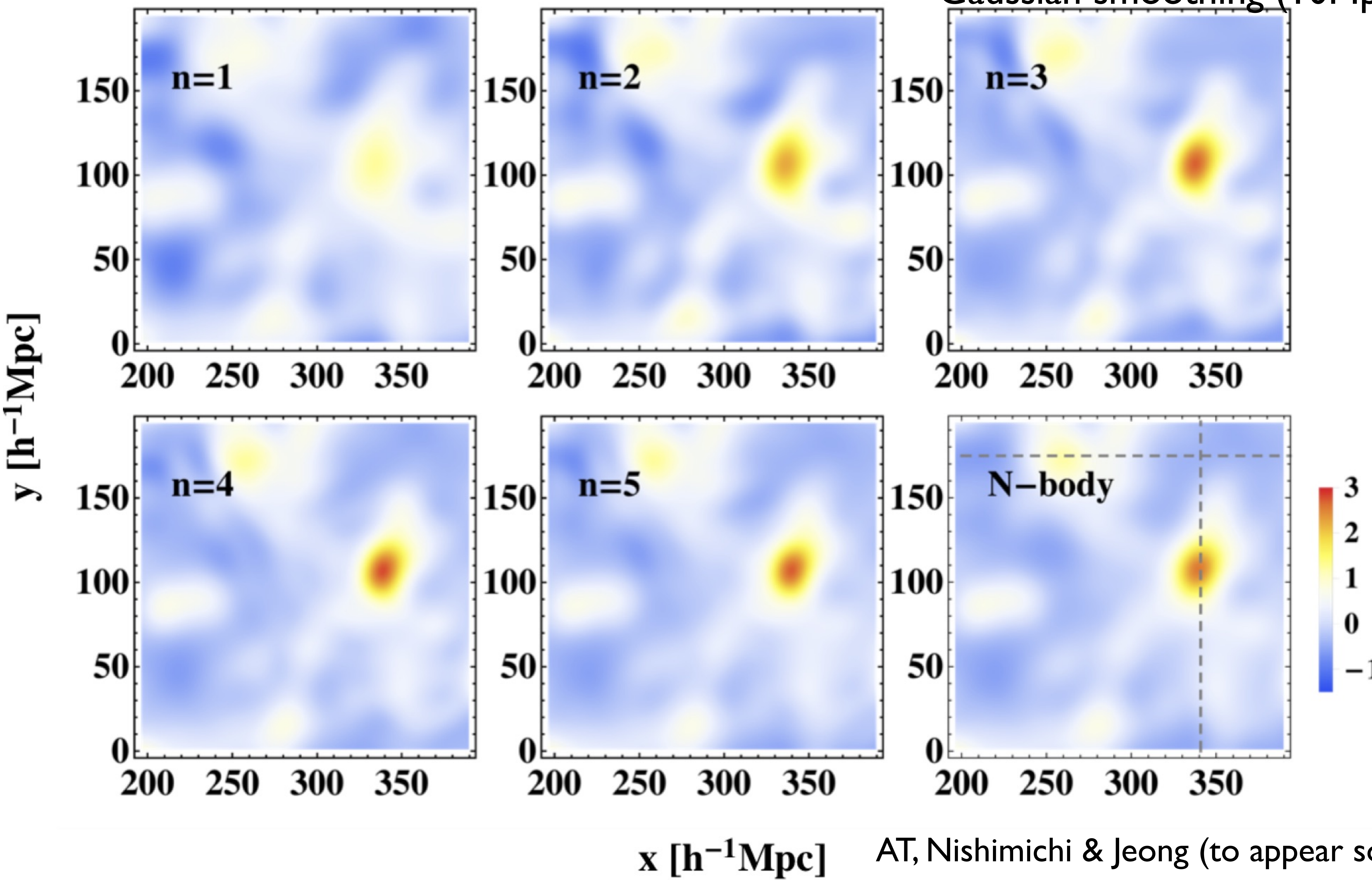

AT, Nishimichi & Jeong (to appear soon)

1D density field in standard PT

Gaussian smoothing (10Mpc/h)

AT, Nishimichi & Jeong (to appear soon)

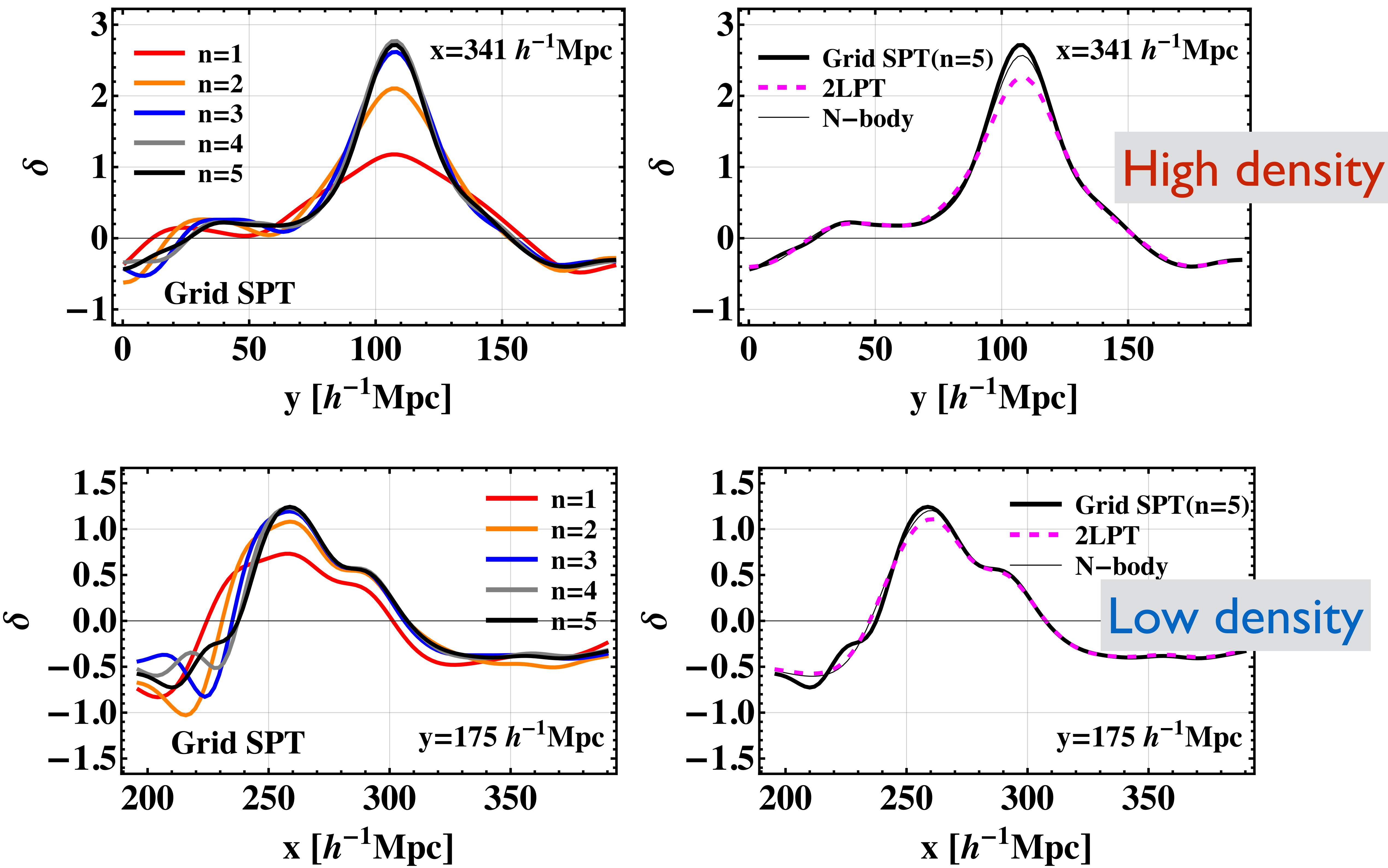

Correlation between N-body and SPT

Gaussian smoothing (10Mpc/h)

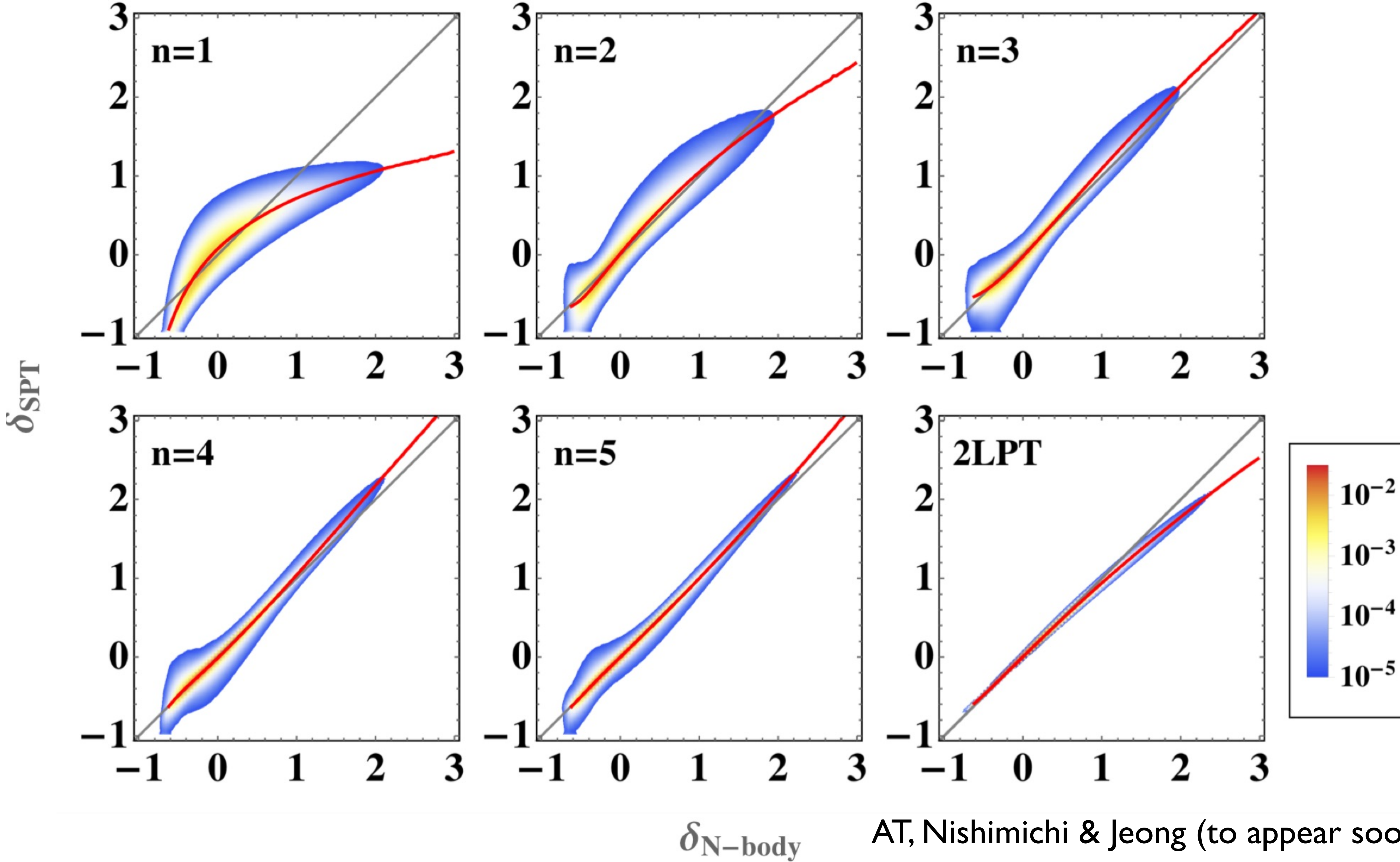

AT, Nishimichi & Jeong (to appear soon)

Improving PT predictions

Basic idea

Reorganizing standard PT expansion by introducing non-perturbative statistical quantities

$\delta_0(\boldsymbol{k})$

initial density field (Gaussian)

$\delta(\boldsymbol{k};z)$

Evolved density field (non-Gaussian)

Initial power spectrum

$P_0(k)$

from linear theory

(CMB Boltzmann code)

Nonlinear mapping

Observables

$P(k;z)$

$B(k_1,k_2,k_3;z)$

$T(k_1,k_2,k_3,k_4;z)$

$\vdots$

of dark matter/galaxies/halos

Concept of '*propagator*' in physics/mathematics may be useful

Propagator in physics

- ✦ Green's function in linear differential equations
- ✦ Probability amplitude in quantum mechanics

Schrödinger Eq.

$$\left(-i\hbar\frac{\partial}{\partial t}+H_x\right)\psi(x,t)=0$$

$$G(x,t;x',t')\equiv\frac{\delta\psi(x,t)}{\delta\psi(x',t')}$$

$$\left(-i\hbar\frac{\partial}{\partial t}+H_x\right)G(x,t;x',t')=-i\hbar\,\delta_D(x-x')\delta_D(t-t')$$

$$\Rightarrow\quad \psi(x,t)=\int_{-\infty}^{+\infty}dx'G(x,t;x',t')\,\psi(x',t')\ ;\quad t>t'$$

Cosmic propagators

Propagator should carry information on
non-linear evolution & statistical properties

Crocce & Scoccimarro ('06)

Evolved (non-linear) density field

$$\left\langle \frac{\delta\,\delta_{\rm m}(\boldsymbol{k};t)}{\delta\,\delta_0(\boldsymbol{k}')} \right\rangle \equiv \delta_{\rm D}(\boldsymbol{k}-\boldsymbol{k}')\,\boxed{\Gamma^{(1)}(k;t)}$$ **Propagator**

Initial density field

Ensemble w.r.t randomness of initial condition

Contain statistical information on *full-nonlinear* evolution

(Non-linear extension of Green's function)

Multi-point propagators

Bernardeau, Crocce & Scoccimarro ('08)
Matsubara ('11) $\longrightarrow$ *integrated PT*

As a natural generalization,

Multi-point propagator

$$\left\langle \frac{\delta^n \, \delta_{\rm m}(\boldsymbol{k};t)}{\delta\,\delta_0(\boldsymbol{k}_1)\cdots\delta\,\delta_0(\boldsymbol{k}_n)} \right\rangle = (2\pi)^{3(1-n)}\,\delta_{\rm D}(\boldsymbol{k}-\boldsymbol{k'})\,\Gamma^{(n)}(\boldsymbol{k}_1,\cdots,\boldsymbol{k}_n;t)$$

With this multi-point prop.

- Building blocks of a new perturbative theory (PT) expansion

  ·········· Γ-expansion or Wiener-Hermite expansion

- A good convergence of PT expansion is expected

  (c.f. standard PT)

Power spectrum

Initial power spectrum

$$P(k;t) = \left[\Gamma^{(1)}(k;t)\right]^2 P_0(k) + 2\int \frac{d^3\boldsymbol{q}}{(2\pi)^3} \left[\Gamma^{(2)}(\boldsymbol{q},\boldsymbol{k}-\boldsymbol{q};t)\right]^2 P_0(q) P_0(|\boldsymbol{k}-\boldsymbol{q}|)$$

$$+ 6\int \frac{d^6\boldsymbol{p}d^3\boldsymbol{q}}{(2\pi)^6} \left[\Gamma^{(3)}(\boldsymbol{p},\boldsymbol{q},\boldsymbol{k}-\boldsymbol{p}-\boldsymbol{q};t)\right]^2 P_0(p)P_0(q)P_0(|\boldsymbol{k}-\boldsymbol{p}-\boldsymbol{q}|) + \cdots$$

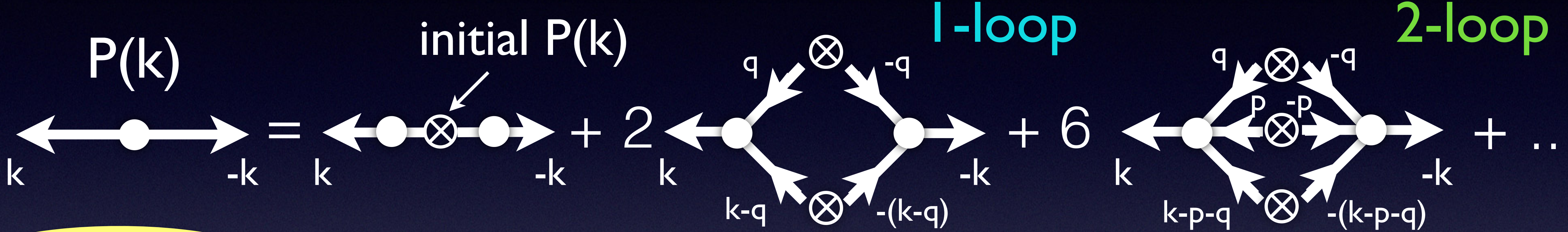

Bispectrum

$$\begin{aligned} B(k_1,k_2,k_3) &= 2\,\Gamma^{(2)}(\mathbf{k}_1,\mathbf{k}_2)\,\Gamma^{(1)}(k_1)\,\Gamma^{(1)}(k_2)\,P_0(k_1)P_0(k_2) + \text{cyc.} \\ &+ \Big[8\int d^3q\,\Gamma^{(2)}(\mathbf{k}_1-\mathbf{q},\mathbf{q})\Gamma^{(2)}(\mathbf{k}_2+\mathbf{q},-\mathbf{q})\Gamma^{(2)}(\mathbf{q}-\mathbf{k}_1,-\mathbf{k}_2-\mathbf{q})P_0(|\mathbf{k}_1-\mathbf{q}|)P_0(|\mathbf{k}_2+\mathbf{q}|)P_0(q) \\ &+ 6\int d^3q\,\Gamma^{(3)}(-\mathbf{k}_3,-\mathbf{k}_2+\mathbf{q},-\mathbf{q})\Gamma^{(2)}(\mathbf{k}_2-\mathbf{q},\mathbf{q})\Gamma^{(1)}(\mathbf{k}_3)P_0(|\mathbf{k}_2-\mathbf{q}|)P_0(q)P_0(k_3) + \text{cyc.}\Big]. \end{aligned}$$

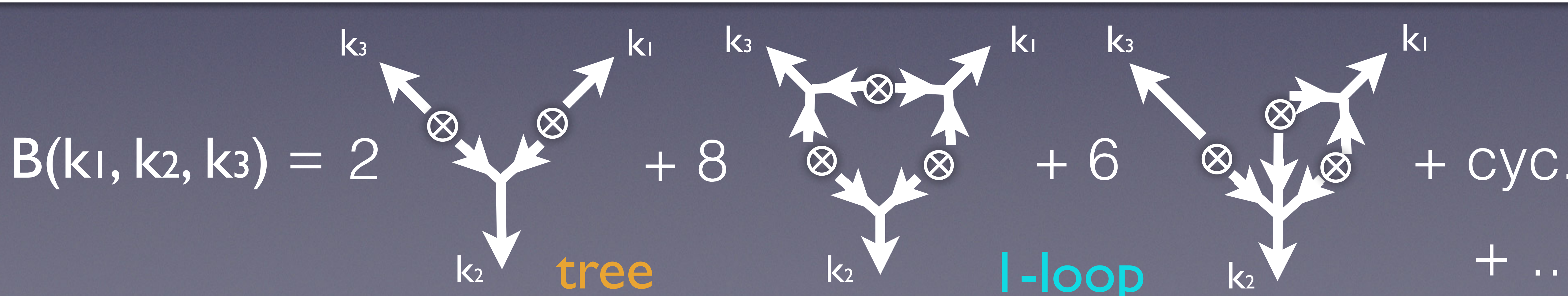

Generic property of propagators

Crocce & Scoccimarro ’06, Bernardeau et al. ’08

$$\Gamma^{(n)} \xrightarrow{k\to+\infty} {}^{s}F_n(\boldsymbol{k}_1,\cdots\boldsymbol{k}_n)\, e^{-k^2\sigma_{\rm v}^2/2} \quad ; \quad \sigma_{\rm v}^2 = \int \frac{dq}{6\pi^2} P_{\theta\theta}(q)$$

$\Gamma^{(1)}(k)$

$\Gamma^{(2)}(k_1,k_2,k_3)$

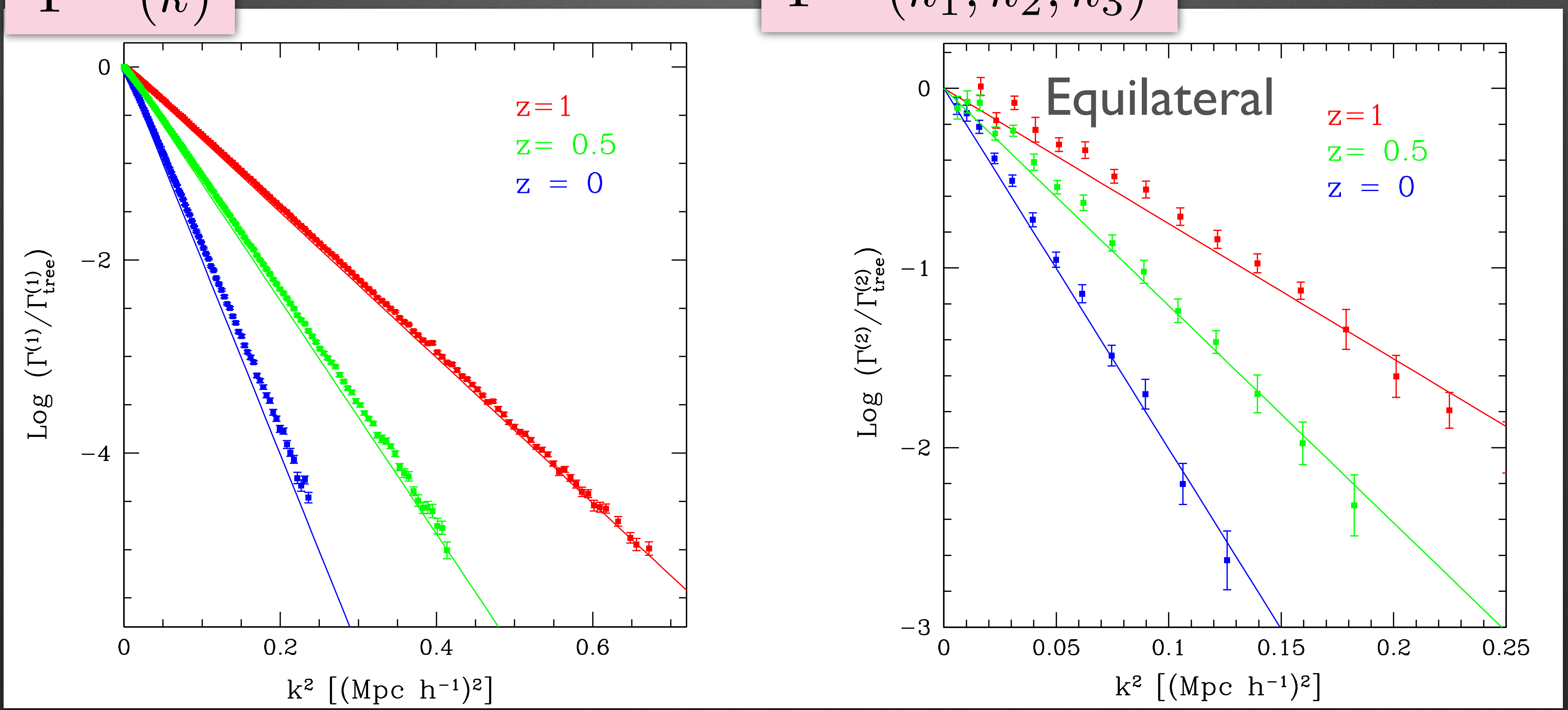

Constructing regularized propagators

- UV property (k >>1) :

$$\Gamma^{(n)} \xrightarrow{k \to +\infty} \Gamma^{(n)}_{\rm tree}\, e^{-k^2\sigma_{\rm v}^2/2} \quad ; \quad \sigma_{\rm v}^2 = \int \frac{dq}{6\pi^2} P_{\theta\theta}(q)$$

Bernardeau, Crocce & Scoccimarro ('08), Bernardeau, Van de Rijt, Vernizzi ('11)

- IR behavior (k<<1) can be described by standard PT calculations :

$$\Gamma^{(n)} = \Gamma^{(n)}_{\rm tree} + \Gamma^{(n)}_{\text{1-loop}} + \Gamma^{(n)}_{\text{2-loop}} + \cdots$$

Importantly, each term behaves like $\Gamma^{(n)}_{p\text{-loop}} \xrightarrow{k \to +\infty} \dfrac{1}{p!}\left(-\dfrac{k^2\,\sigma_{\rm v}^2}{2}\right)^p \Gamma^{(n)}_{\rm tree}$

➡ A regularization scheme that reproduces both UV & IR behaviors

Bernardeau, Crocce & Scoccimarro ('12)

Regularized propagator

Bernardeau, Crocce & Scoccimarro ('12)

A global solution that satisfies both UV (k>>1) & IR (k<<1) properties:

$$\Gamma^{(n)}_{\rm reg} = \left[\Gamma^{(n)}_{\rm tree}\left\{1+\underbrace{\frac{k^2\sigma_{\rm v}^2}{2}}_{\text{counter term}}\right\} + \Gamma^{(n)}_{\text{1-loop}}\right]\exp\left\{-\frac{k^2\sigma_{\rm v}^2}{2}\right\}; \quad \sigma_{\rm v}^2 = \int\frac{dq}{6\pi^2}P_{\theta\theta}(q)$$

.... *IR behavior is valid at 1-loop level*

Precision of IR behavior can be systematically improved by including higher-loop corrections and adding counter terms

e.g., For IR behavior valid at 2-loop level,

$$\Gamma^{(n)}_{\rm reg} = \left[\Gamma^{(n)}_{\rm tree}\left\{1+\underbrace{\frac{k^2\sigma_{\rm v}^2}{2}+\frac{1}{2}\left(\frac{k^2\sigma_{\rm v}^2}{2}\right)^2}_{\text{counter term}}\right\} + \Gamma^{(n)}_{\text{1-loop}}\left\{1+\underbrace{\frac{k^2\sigma_{\rm v}^2}{2}}_{\text{counter term}}\right\} + \Gamma^{(n)}_{\text{2-loop}}\right]\exp\left\{-\frac{k^2\sigma_{\rm v}^2}{2}\right\}$$

Propagators in N-body simulations

compared with '*Regularized*' propagators constructed analytically

$\Gamma^{(1)}(k)$ predictions up to 2-loop order

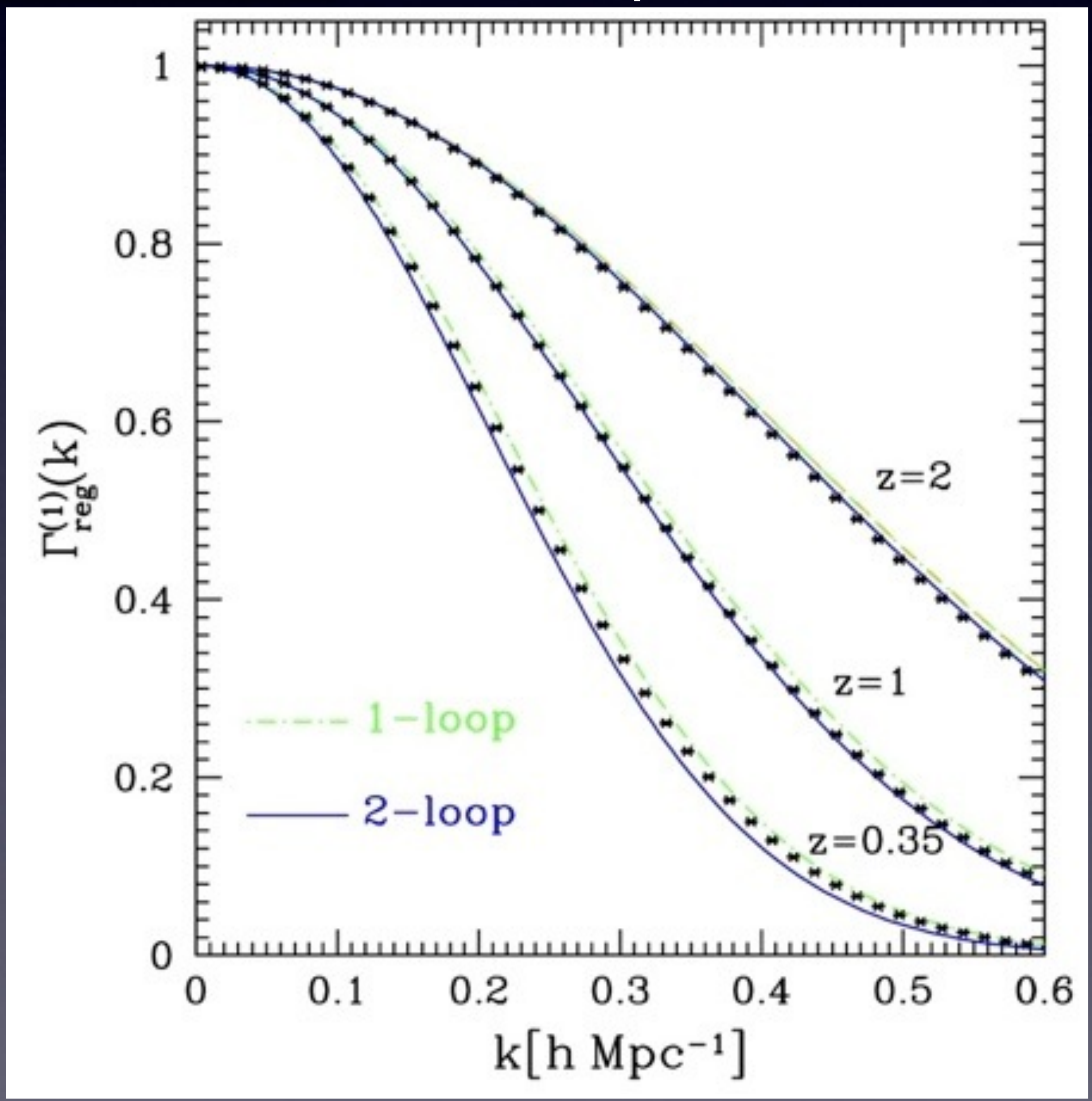

Bernardeau, AT & Nishimichi ('12)

$\Gamma^{(2)}(k_1, k_2, k_3)$ predictions up to 1-loop order

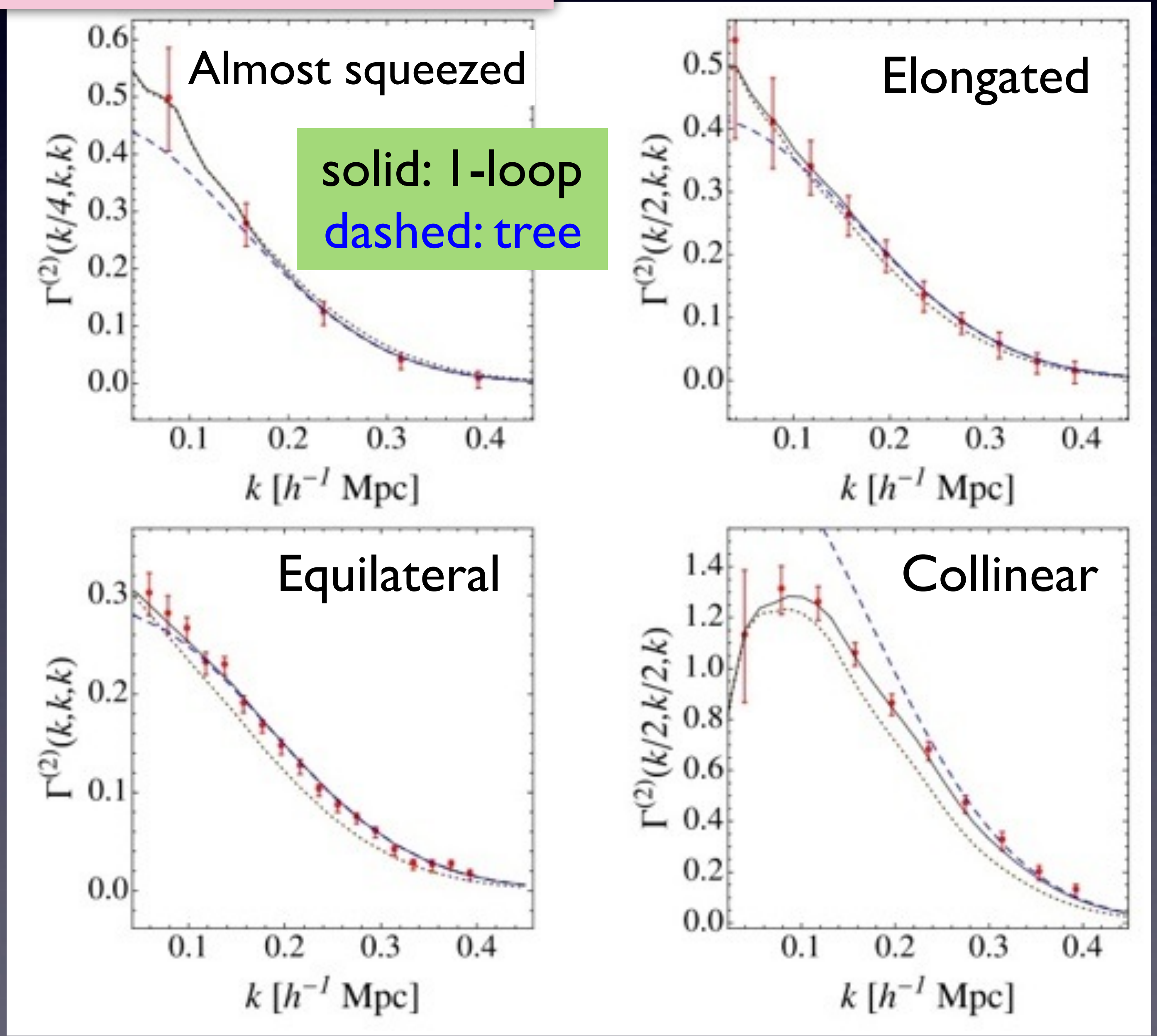

Bernardeau et al. ('12)

RegPT: fast PT code for P(k) & ξ(r)

few sec.

(regularized)

A public code based on multi-point propagators at *2-loop order*

http://www2.yukawa.kyoto-u.ac.jp/~atsushi.taruya/regpt_code.html

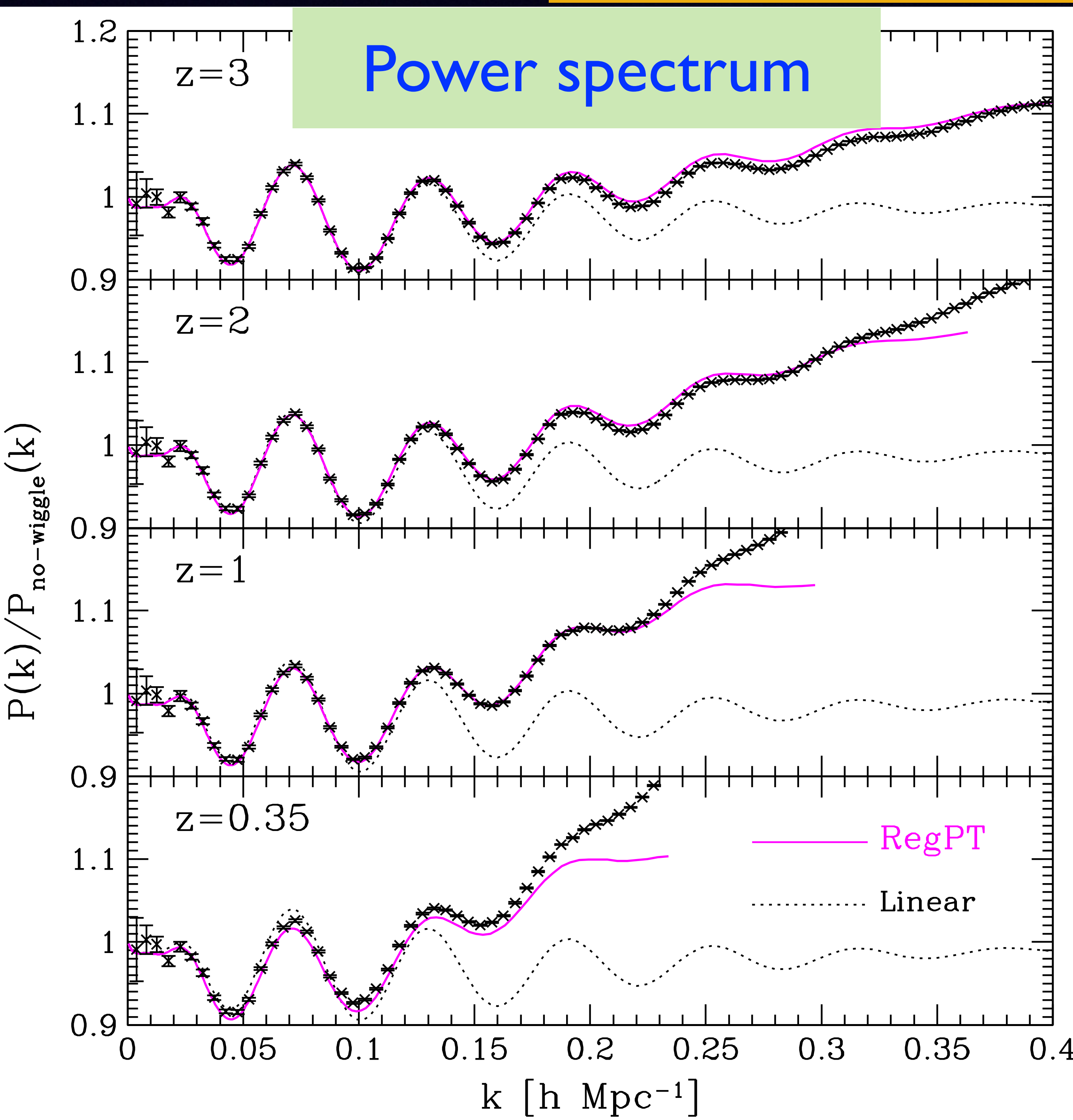

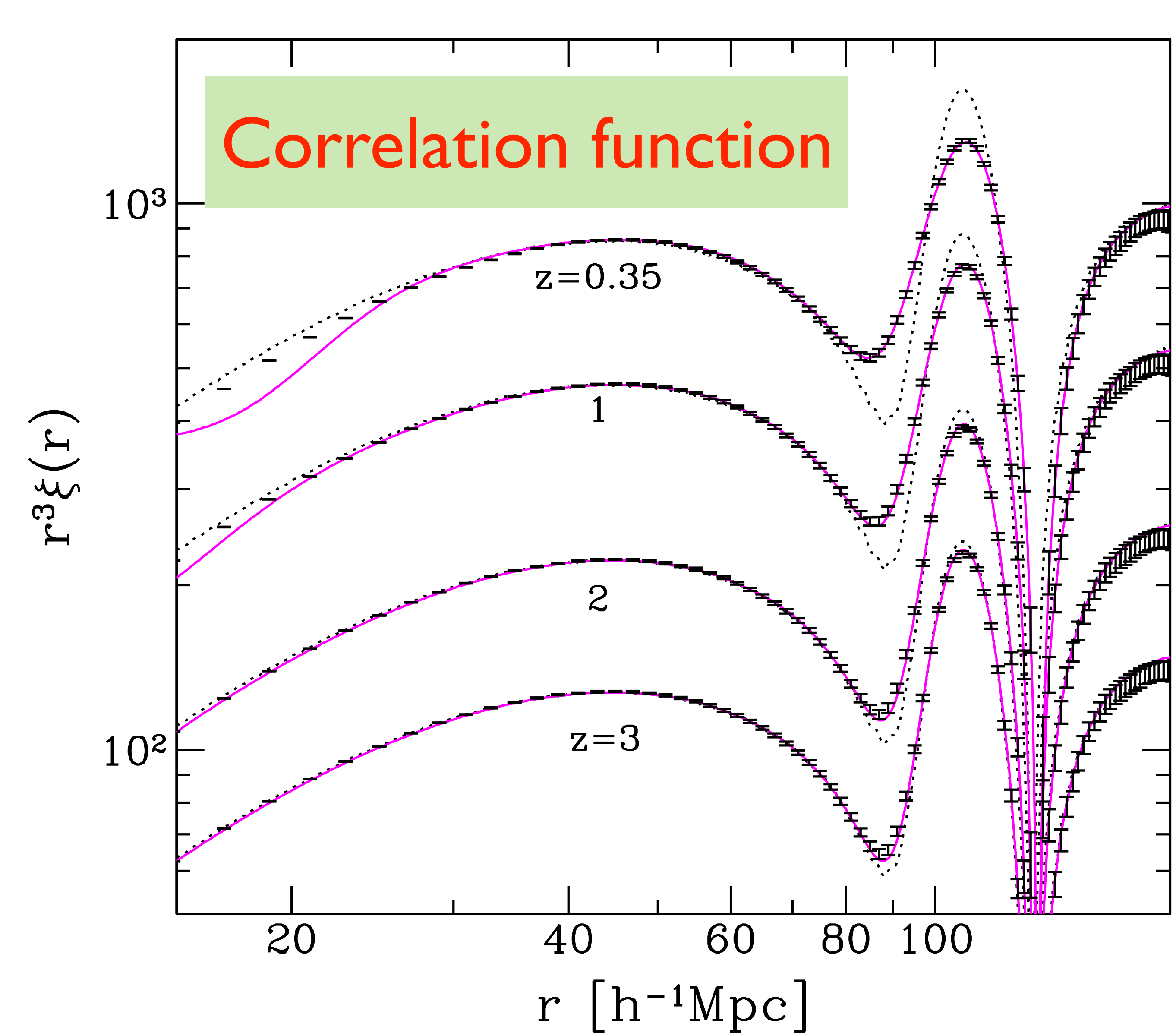

AT, Bernardeau, Nishimichi & Codis ('12)

Why improved PT works well?

AT, Bernardeau, Nishimichi, Codis ('12)
AT et al. ('09)

- All corrections become comparable at low-z.
- Positivity is not guaranteed.

Corrections are positive & localized, shifted to higher-k for higher-loop

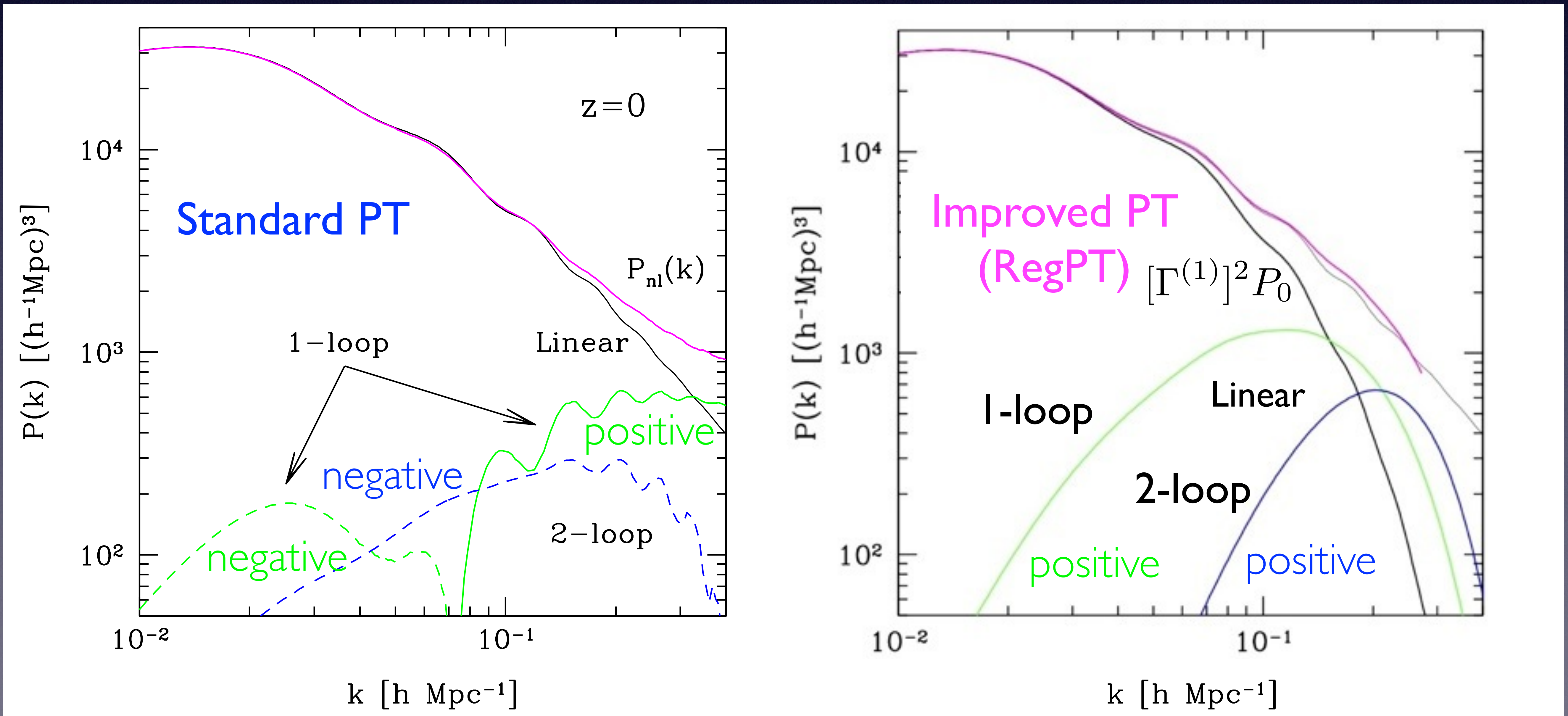

RegPT in modified gravity

Good convergence is ensured by
a *generic* damping behavior in propagators $\Gamma^{(n)} \xrightarrow{k\to\infty} \Gamma^{(n)}_{\rm tree}\, e^{-k^2\sigma_{\rm d}^2/2}$

Even in modified gravity, well-controlled expansion with RegPT

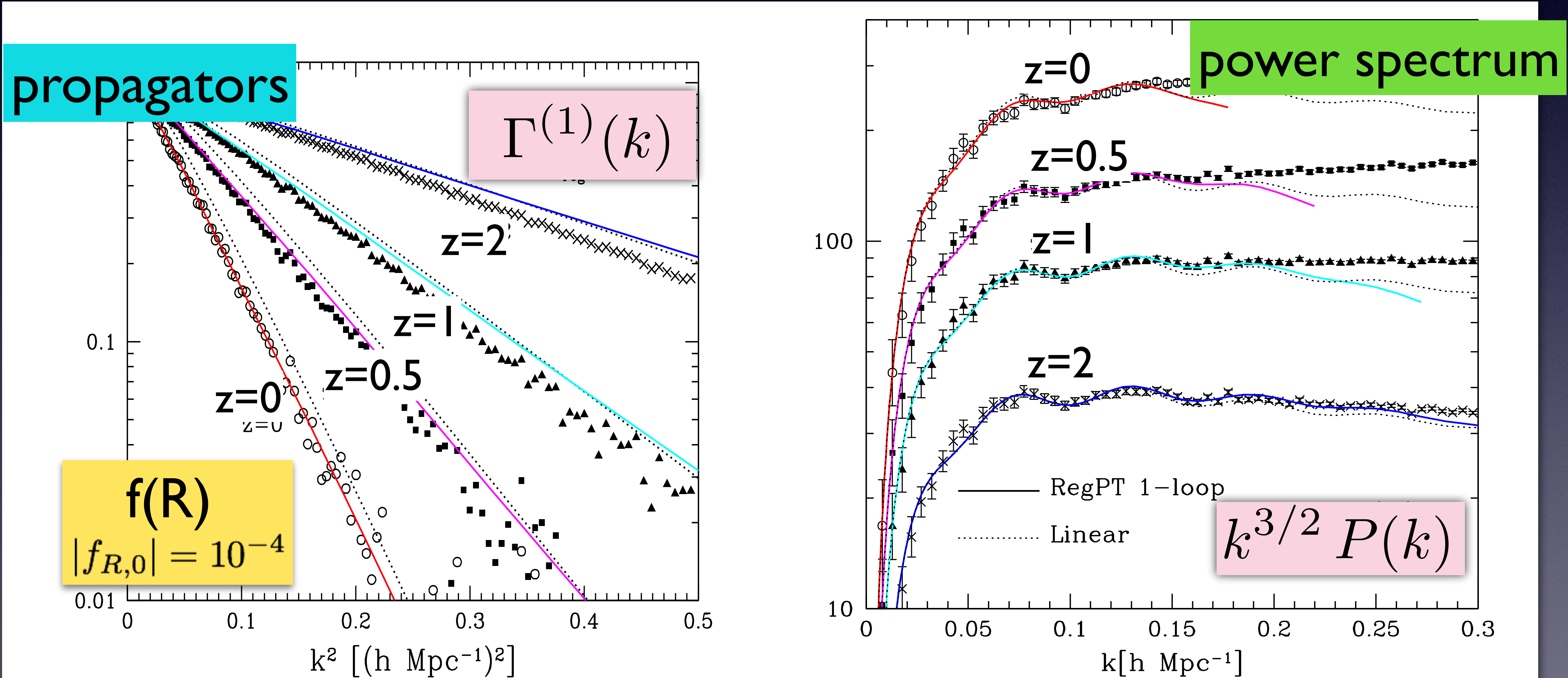

N-body data: Baojiu Li

AT, Nishimichi, Bernardeau,et al.('14)